ISTANBUL TECHNICAL UNIVERSITY ★ GRADUATE SCHOOL OF SCIENCE ENGINEERING AND TECHNOLOGY

EVALUATION OF AN AUTOMOTIVE AIR INTAKE SYSTEM IN TERMS OF PRESSURE LOSS AND FLOW CHARACTERISTICS

M.Sc. THESIS

Anıl Can AĞAR

Department of Mechanical Engineering

Heat Transfer-Fluid Mechanics Programme

Thesis Advisor: Prof. Dr. İ. Bedii Özdemir

SEPTEMBER 2015

ISTANBUL TECHNICAL UNIVERSITY ★ GRADUATE SCHOOL OF SCIENCE ENGINEERING AND TECHNOLOGY

**EVALUATION OF AN AUTOMOTIVE AIR INTAKE SYSTEM
IN TERMS OF
PRESSURE LOSS AND FLOW CHARACTERISTICS**

M.Sc. THESIS

**Anıl Can AĞAR
(503101101)**

Department of Mechanical Engineering

Heat Transfer-Fluid Mechanics Programme

Thesis Advisor: Prof. Dr. İ. Bedii Özdemir

SEPTEMBER 2015

İSTANBUL TEKNİK ÜNİVERSİTESİ ★ FEN BİLİMLERİ ENSTİTÜSÜ

**BİR ARAÇ HAVA EMİŞ SİSTEMİNİN
BASINÇ KAYIPLARI VE AKIŞ KARAKTERİSTİKLERİ
AÇISINDAN İNCELENMESİ**

YÜKSEK LİSANS TEZİ

**Anıl Can AĞAR
(503101101)**

Makina Mühendisliği Anabilim Dalı

Isı-Akışkan Yüksek Lisans Programı

Tez Danışmanı: Prof. Dr. İ. Bedii Özdemir

EYLÜL 2015

Anıl Can Ağar, a M.Sc. student of ITU Graduate School of Science Engineering and Technology student ID 50310101, successfully defended the thesis entitled "EVALUATION OF AN AUTOMOTIVE AIR INTAKE SYSTEM IN TERMS OF PRESSURE LOSS AND FLOW CHARACTERISTICS", which he prepared after fulfilling the requirements specified in the associated legislations, before the jury whose signatures are below.

Thesis Advisor :	**Prof. Dr. İ. Bedii ÖZDEMİR** İstanbul Technical University	....
Jury Members :	**Öğr. Gör. Dr. Orhan ATABAY** İstanbul Technical University	....
	Yrd. Doç. Dr. Özgür ERTUNÇ Özyeğin University	....

Date of Submission : 03 September 2015
Date of Defense :   18 September 2015

To all those made this study possible, to friends and family,

FOREWORD

I cannot thank enough to my supervisor Prof. Dr. İlyas Bedii Özdemir, who shared his valuable information and expert opinion throughout the study. He believed in the study and provided any kind of guidance whenever it is needed.

x

TABLE OF CONTENTS

ABBREVIATIONS

AIS   **:** Air Intake System
CFD   **:** Computational Fluid Dynamics
FVM   **:** Finite Volume Method
PDE   **:** Partial Differential Equation
SIMPLE   **:** Semi Implicit Method for Pressure Linked Equations ASTM
ASTM   **:** American Society for Testing and Materials

LIST OF TABLES

LIST OF FIGURES

NOMENCLATURE

$\boldsymbol{\rho}$	**:** density
$\vec{\boldsymbol{v}}$	**:** velocity vector
$\vec{\boldsymbol{a}}$	**:** surface normal vector
$\boldsymbol{S_u}$	**:** net mass generated inside volume element
$\otimes$	**:** tensor (dyadic) product
$\boldsymbol{I}$	**:** identity matrix
$\boldsymbol{\tau}$	**:** viscous flux tensor
$\overrightarrow{\boldsymbol{f_p}}$	**:** body force per volume caused by porous media
$\boldsymbol{\mu_{eff}}$	**:** effective viscosity
$\boldsymbol{\mu}$	**:** laminar viscosity
$\boldsymbol{\mu_{t'}}$	**:** turbulent viscosity
$\boldsymbol{C_\mu}$	**:** realizable k-epsilon coefficient
$\boldsymbol{\kappa}$	**:** turbulent kinetic energy
$\boldsymbol{\varepsilon}$	**:** turbulent dissipation rate
$\boldsymbol{P_v}$	**:** porous viscous resistance tensor
$\boldsymbol{P_i}$	**:** porous inertial resistance tensor
$\boldsymbol{H}$	**:** total enthalpy
$\overrightarrow{\dot{\boldsymbol{q}}''}$	**:** heat flux vector
$\boldsymbol{k_{eff}}$	**:** effective thermal conductivity
$\boldsymbol{\chi}$	**:** porosity
$\boldsymbol{k_{solid}}$	**:** solid region's thermal conductivity
$\boldsymbol{k_{fluid}}$	**:** effective thermal conductivity for turbulent flows
$\boldsymbol{k}$	**:** thermal conductivity of the fluid
$\boldsymbol{C_p}$	**:** specific heat
$\boldsymbol{Pr_{t'}}$	**:** turbulent Prandtl number
$\vec{\boldsymbol{v}}*$	**:** intermediate velocity vector field
$\dot{\boldsymbol{m}}_f*$	**:** uncorrected mass fluxes at faces
$\boldsymbol{p}'$	**:** pressure correction
$\boldsymbol{\omega}$	**:** under-relaxation factor for pressure
$\boldsymbol{p'_b}$	**:** boundary pressure corrections
$\nabla \boldsymbol{p}'$	**:** gradient of the pressure corrections
$\boldsymbol{a'^v_p}$	**:** vector of central coefficients
$\boldsymbol{V}$	**:** cell volume
$\nabla \boldsymbol{P}$	**:** pressure gradient
$\boldsymbol{\alpha}$	**:** permeability coefficient
$\boldsymbol{v}$	**:** Darcy velocity

EVALUATION OF AN AUTOMOTIVE AIR INTAKE SYSTEM IN TERMS OF PRESSURE LOSS AND FLOW CHARACTERISTICS

SUMMARY

In diesel engines, determination of pressure losses on air intake system is of crucial importance due to its detrimental effect on engine performance. Inefficiencies in performance present itself in elevated fuel consumption and/or high emmisions. Main effect of pressure losses in air intake system (AIS) is on compressor performance and combustion efficiency. The term AIS includes a major portion of an internal combustion engine's air path. In internal combustion engines, air path is basically a series of closed conduits that starts from grill opening that collects the fresh air to the exhaust tailpipe. AIS is the common name for system that comprises group of engine components which are responsible to deliver fresh air into the combustion chamber. Area of interest in this study is the series of components conveying air from atmosphere until compressor. Parts included in this study are the portion of AIS from atmosphere until compressor; a grill opening, dirty side ducts, air filter assembly, clean side ducts.

When high pressure losses occur inside this system, AIS can accommodate less fluid flow under existing operating conditions to fulfil the demand of charged air into combustion chamber, compressor is forced to work in an inefficient operating point, resulting in extra load to turbine. Excessive load on turbine increases back pressure and hence, this phenomenon diminishes the combustion performance. To choose and calibrate the related parts of AIS, such as turbocharger, intake manifold, pressure losses from upstream should be determined correctly. However, this determination should be performed in early stages of design, leading to difficulties and complexity for test. Hence, employing a computational fluid dynamics (CFD) solver is more than a necessity to perform such evaluation. Yet again, to conduct a CFD study and to achieve reliable results in good correlation with real operating conditions, most of the cases require a validation procedure that includes testing.

In this study a valid evaluation of the AIS performance is aimed. To achieve this goal, objectives that followed is;

- Acquiring information about AIS system boundary conditions,

- Building a CFD Model to model air filter's pressure loss characteristics,

- Comparing pressure loss obtained in CFD model with ASTM (American Society for Testing and Materials) F778 Standard Air Permeability test results,

- Building sector CFD models to evaluate the behavior of the filter element when installed into air filter assembly,

- Quantifying filter behavior with results of sector analyses and determining porous media tensor to represent filter element in complete AIS CFD model,

- Building a full CFD model including all low pressure portion of the AIS and evaluating flow performance in terms of pressure loss and flow characteristics such as flow uniformity values on before and after mass flow rate sensor, filter element and at compressor inlet.

- Gathering test results for the AIS subjected to CFD analyses and comparing pressure loss behavior to validate the evaluation.

To perform CFD Analyses, a commercial CFD Solver called StarCCM+ (v.10.02) is used for analyses. Upon completion of the study, findings collected are as follows:

- ASTM F778 test is reproduced via CFD, calculating air filter element's pressure loss with less than 7% difference in comparison with measurement.

- CFD analysis of AIS is underpredicting the pressure loss by 11% when compared to tests.

- CFD analysis of AIS underpredicts the pressure loss value around 15% for pleated air filter element when compared to measurement data.

The results can be considered satisfactory, as the method to evaluate pressure loss is applicable for early stages of design where it is too expensive and time consuming to build and test a prototype for each design. Besides, the values of deviation for each pressure loss value are lesser than similar studies in literature, due to the increased detail level and quality.

BİR ARAÇ HAVA EMİŞ SİSTEMİNİN BASINÇ KAYIPLARI VE AKIŞ KARAKTERİSTİKLERİ AÇISINDAN İNCELENMESİ

ÖZET

Bir otomobilin tasarımındaki en önemli unsurlardan biri üretilen parçaların akışkanlarla etkileşiminin doğru şekilde hesaplanması ve davranışının önceden bilinmesidir. Özellikle araca hareket fonksiyonunu kazandıran motor, akışkan etkileşimi bakımından tüm aracın en karmaşık kısmıdır. Sistemdeki sürtünmeyi azaltan yağlama sistemindeki yağın, yanma sonucu ortaya çıkan ısının malzeme için tehlikeli olmasını önleyen soğutma sistemindeki suyun, yanma odasına beslenen yakıtın ve en önemlisi atmosferden yanma odasına, yanma odasından eksoza gerçekleşen ve motor performansını belirleyen havanın akışı, motor içerisindeki akışkan hareketlerini oluşturur. Bu çalışmanın ana odağında havanın atmosferden yanma odasına kadar izlediği yolu oluşturan hava emiş sistemi bulunmaktadır. Hava emiş sistemindeki kayıpların hesaplanması ve tasarımın kayıpları en aza indirecek şekilde yapılması motorun tasarımı açısından kritik önem taşır. Son yıllarda daha çevreci motorlar üretilmesi yönünde yapılan yasal düzenlemeler, otomotiv şirketlerini üretilen her motordan olabilecek en iyi performansı ve en yüksek verimi almaya yönlendirmektedir. Günümüz teknolojisinde hava emiş sisteminde karşılaşılan karmaşık geometri ve yapıların üç boyutlu hesaplamalı akışkanlar dinamiği (HAD) ile incelenip performansının değerlendirilmesi mümkündür. Bu çalışmada hava emiş sisteminin akışkanlar dinamiği açısından en karmaşık parçası sayılabilecek hava filtresinin HAD ile modellenmesini kolaylaştıran bir yöntem geliştirilmiş ve kullanıma sunulmuştur.

Hava emiş sistemindeki kayıpların doğru hesaplanabilmesi için otomotiv firmaları iki ana yol izlemektedirler. Bunlardan birincisi hava ile etkileşecek parçaların prototiplerinin üretilerek deneylere tabi tutulması olup bu yöntem çoğunlukla motor tasarımının ilk aşamalarında mümkün değildir. Bu yöntemin kullanılması aynı zamanda birden fazla tasarım alternatifinin değerlendirilmesi gerektiği durumlarda oldukça pahalı ve iş gücü gerektiren bir hal alır. Bu güçlükleri içermeyen ve tasarım esnasında kullanılan diğer yöntem ise bilgisayar destekli benzetimlerle parçaların performanslarının sanal ortamda değerlendirilmesidir. İçerdiği karmaşıklık ve gerektirdiği teorik bilgi yükü nedeniyle benzetimin doğru, gerçeğe yakın ve etkin şekilde yapılması sistem hakkında doğru bilgiyi almak açısından büyük önem taşır.

Hesaplamalı akışkanlar dinamiği açısından hava emiş sisteminin en karmaşık parçası içerdiği küçük ölçekli detaylar ve gözenekli yapısı nedeniyle hava filtresidir. Otomobillerde kullanılan hava filtreleri çoğunlukla "filtre kağıdı" adı verilen geniş düzlemsel malzemenin katlanması ile elde edilen girinti ve çıkıntılara sahip geometriyi içerir. Bu parçanın ana görevi aracın çalıştığı ortamdaki tozun ve kirin motorun içerisine ulaşmasını önlemektir. Motorun çalışması esnasında iyi tasarlanmış bir hava emiş sistemi üzerindeki kayıpların büyük çoğunluğunu hava filtresi oluşturur. Kaybın HAD ile doğru hesaplanabilmesi için filtrenin karmaşık

yapısının doğru modellenmesi esastır. Ancak hava filtresinin en ince ayrıntısına kadar modellenmesi benzetime çok büyük bir hesaplama yükü getirir. Bu nedenle literatürdeki genel eğilim, hava filtresinin detaylardan arındırılarak gözenekli bir blok halinde modellenmesi yönündedir. Hava emiş sisteminin tümünün benzetime katıldığı durumlarda bu yaklaşımın hesaplama süresi ve maliyeti bakımından getirdiği kazanımlar aşikardır. Ancak bahsi geçen "gözenekli blok" model içerisinde doğru temsil edilmelidir. Ticari HAD programları genellikle gözenekli ortamın yarattığı kayıpları genel momentum denkleminde gövde kuvveti adı verilen momentum kayıp mekanizmaları altında değerlendirir.

Bu çalışmanın amaçlarından biri benzetimde kullanılan momentum denklemindeki gövde kuvvetinin doğru hesaplanmasını sağlamada kullanılan katsayıları belirlemede kullanılan bir yöntemin başarıyla uygulanmasıdır. Bu yöntem fiziksel özellikleri bilinen karmaşık hava filtresi geometrisinin küçük bir kısmının analiz edilmesi sayesinde, deneysel yöntemler kullanılmaksızın yeterli bir yaklaşıklıkla ilgili katsayıların hesaplanmasını sağlamaktadır. Çalışmaya konu olan düzlemsel hava filtresi içerisinden seçilen alan, filtre kağıdında oluşan üç ana yöndeki akış HAD analizine tabi tutulmuştur. Bu üç ana yön; havanın katlamaların gerçekleştirildiği doğruya paralel doğrultu, havanın büyük çoğunluğun izlediği yol olan katlama doğrultusuna düşey yönde dik olan doğrultu ve havanın geçmekte en çok zorlanacağı katlamalara filtre düzleminde dik olan doğrultudur. Bu üç doğrultu üç ayrı benzetim grubunda incelenmiş ve her benzetimde o doğrultuya özgü tahmini debi aralıkları taranarak hızlara bağlı basınç kaybı karakteristikleri belirlenmiştir. Belirlenen bu değerler üzerinden geçirilen eğrilerle Forchaimer terimini içeren Darcy kanununa göre poroz ortam katsayılarına ulaşılmıştır. Benzetimlerde yaygın kullanılan ticari HAD yazılımlarından StarCCM+(v10.02) tercih edilmiştir.

Üç ana yönde yapılan analizler sonucunda elde edilen gözenekli ortama dair katsayılar daha sonra benzetime tabi olan filtre kağıdının takıldığı bütün bir hava emiş sisteminin analizinde kullanılmış ve sistemde oluşan basınç kayıpları kademeli bir şekilde hesaplanmıştır. Çalışma sonunda hesaplanan basınç kayıpları ilgili standart yönergelere uygun yapılmış deneylerle doğrulanmıştır.

Doğru bir hava emiş sistemi modellemesi için HAD modelinin yalnızca basınç kaybını doğru modellemesi de yeterli değildir. Yapılan benzetimde gözenkli blok halinde modellenen filtre kağıdı bölgesinin içerisinde oluşacak akış alanının doğru şekilde modellenmesi de öncesindeki ve sonrasındaki parçaların oluşturduğu kayıpları doğru modellemek açısından kritik önem taşımaktadır.

Bu yöntem ile daha önceden yapılan deneyler ile belirlenen gözenekli ortam katsayıları deneye ihtiyaç duymaksızın HAD ile belirlenebilir hale gelmiştir. Yöntemin etkin çalışabilmesi için gereken tek deney otomotiv ve tekstil endüstrisinde filtre elemanlarının standartlaştırılması amacıyla yapılan ASTM(F778-88) standartlarına dayalı ölçümün sonuçlarıdır. Filtre kağıdı üreticileri ürün gamındaki ürünleri bu deney ile belirlenen hava geçirgenliğine göre sınıflandırırlar. Seçilen filtre için ulaşılan hava geçirgenliği ölçüm sonuçlarına da çalışma içerisinde ayrıca yer verilmiştir.

Çalışmanın tamamlanması ile beraber;
  - Hava emiş sisteminin basınç kaybı ölçülen değere kıyasla HAD tarafından %11 seviyesinde bir fark ile doğru tahmin edilmiştir.
  - Hava filtre elemanının katlanmış haldeki basınç kaybı HAD tarafından, ölçülen değerine kıyasla %15 daha az olarak tahmin edilmiştir.

- ASTM F778-88 standardı kapsamında yapılan ölçüm HAD ortamında tekrarlanmış ve basınç kaybı %7'nin altında bir fark ile doğru tahmin edilmiştir.

Filtre elemanının HAD benzetimlerinde daha detaylı incelenmesi sayesinde basınç kayıpları literatürdeki benzer çalışmalara kıyasla daha ölçüm sonuçlarına daha yüksek yaklaşıklıkla belirlenmiştir.

Bunun yanı sıra kütle debisi sensörünün öncesi ve sonrası, filtre elemanının giriş yüzeyi, kompresör girişi gibi kritik bölgelerdeki akış dağılımları görsel olarak alınan eş basınç ve hız eğrileri ile; ve sayısal olarak da tekdüzelik katsayısı (uniformity index) ile gösterilmiştir.

1. INTRODUCTION

The term Air Intake System (AIS) includes a major portion of an internal combustion engine's air path. In internal combustion engines, air path is basically a series of closed conduits that starts from grill opening that collects the fresh air to the exhaust tailpipe. AIS is the common name for pack of parts that has fresh air inside. As can be seen in Figure 1.1, AIS includes all the pipeline until air enters into the combustion chamber.
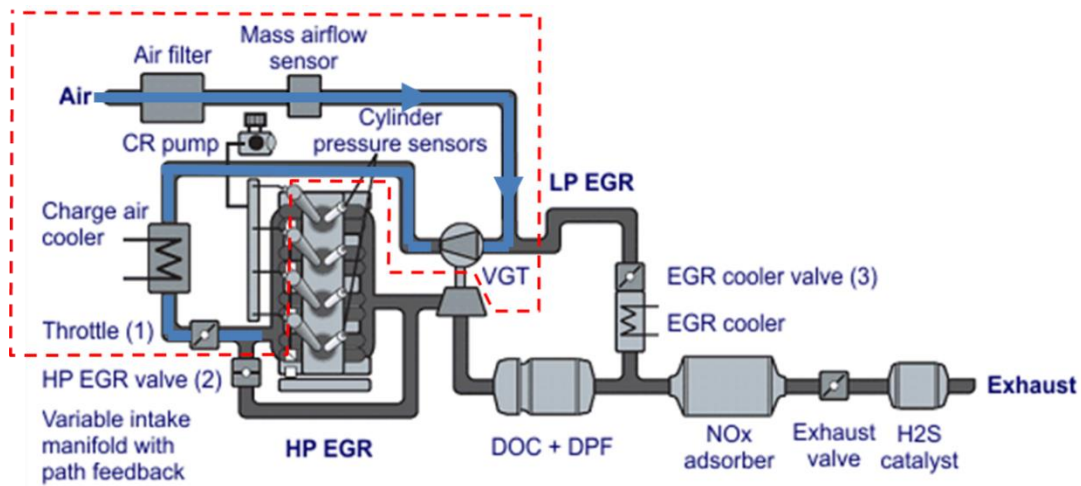
Figure 1.1 : Schematic view of an automotive AIS [1]

This study is performed on a diesel engine that includes air charging subsystem. Air charging subsystem generally comprises a compressor for pressurizing the fresh air fed to combustion chamber. As can be seen in block diagram given in Figure 1.2, typical components of the AIS include a grill opening, intake ducts (dirty side ducts), air filter, clean side ducts, a compressor, hot charged ducts, a charge air cooler, cold charged ducts, throttle body and intake manifold.

In Figure 1.2, the portion of AIS called 'Low pressure ducts' is marked as the area of interest. In this study, the flow characteristics and pressure losses of this region will be inspected in depth.

Figure 1.2 : Area of interest inside AIS.

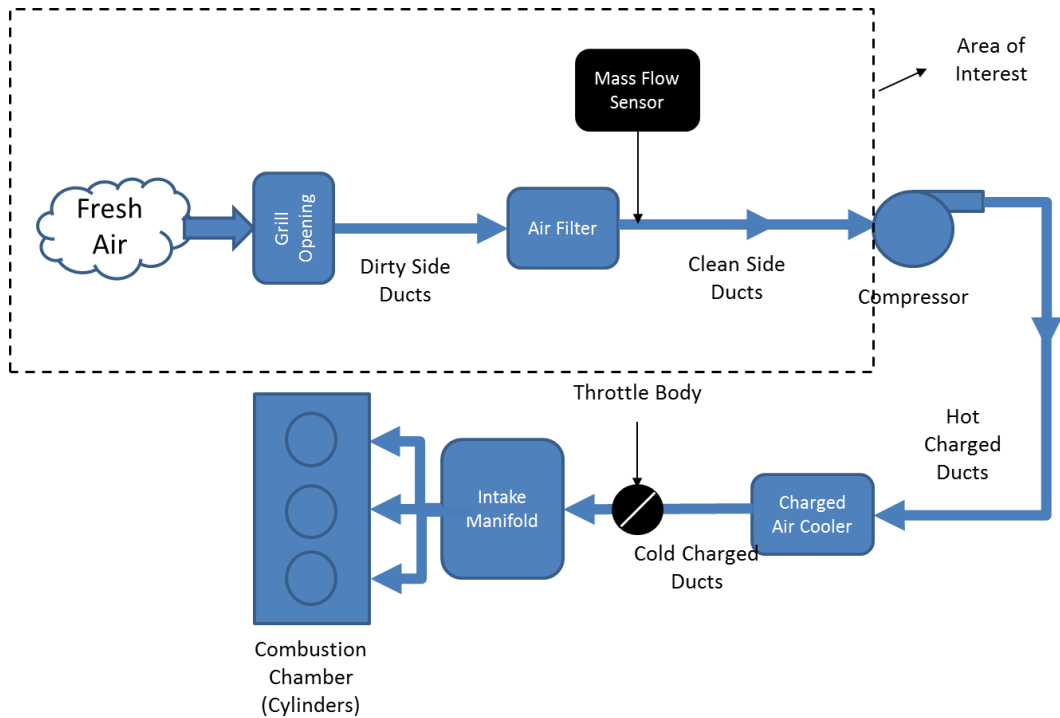Determination of pressure losses and flow behavior in AIS is crucial due to the effects on engine performance. Flow characteristics of AIS is needed to be obtained in early stages of the engine design for hardware selection for numerous essential engine components including; compressor, mass flow sensor, charged air cooler.

There are two main paths that can be followed for assessing performance of the AIS which are conducting tests and building CFD models.

Building a CFD model to represent flow behavior, can return approximate results in a fast and relatively cheaper manner. Hence, employing a CFD solver is more than a necessity to perform such evaluation.

However, a robust and representative CFD model for entire AIS must include a valid method to evaluate air filter flow characteristics. Due to the fact that filter can have an extremely complex geometry with large and small scales and microstructure in filter element is non-deterministic, modelling of air filter is one of the most difficult problems to solve with current technology. Figure 1.3 shows the typical filter element geometry which causes most of the complexity for CFD analyses of AIS.
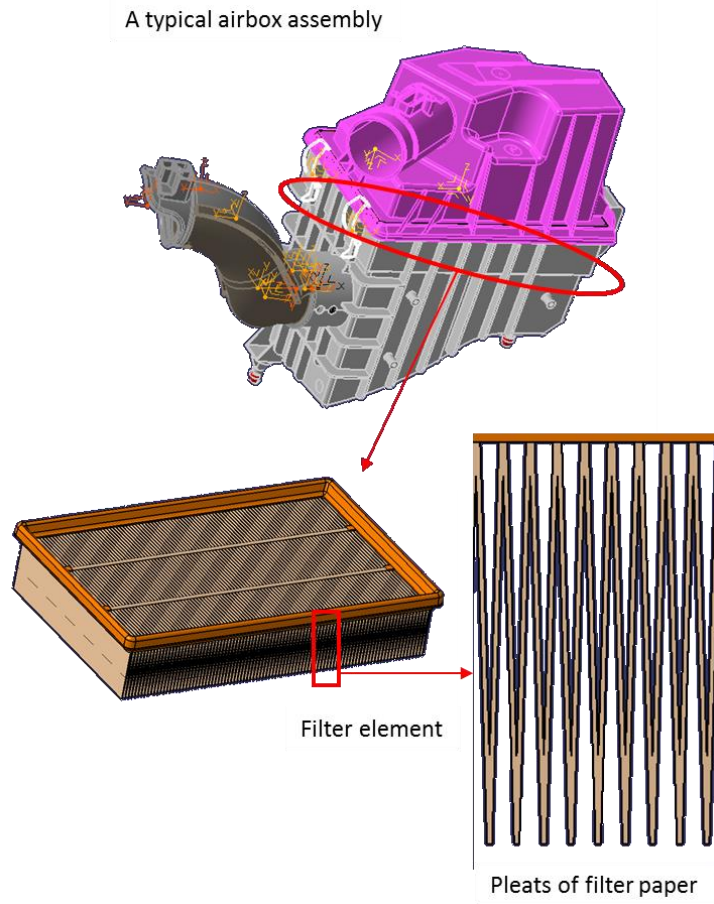
Figure 1.3 : A typical Air Filter Box Assembly [2]

1.1 Purpose of Thesis

For vehicles of all size, AIS is one of the most crucial systems for engine operation. The robustness of design affects a wide variety of engine performance parameters including compressor efficiency, compressor noise, fuel consumption, combustion efficiency, emission levels. In addition, for the engine subjected to this study, there are extra requirements such as targets that are needed to be achieved for mass flow sensor to work without loss of fidelity, flow uniformity level to be attained in the front face of the filter element.

Main purpose and motivation behind this study is to deliver a robust and reliable AIS design that is in full compliance with prescribed targets and performance metrics. In order to achieve this goal there are several objectives to be attained. These objectives include;

- Acquiring information about boundary conditions corresponding worst case scenario for AIS,
- Predicting filter's pressure loss characteristics via a CFD model,
- Comparing pressure loss obtained in CFD model with ASTM F778 Standard Air Permeability test results,
- Building sector CFD models to evaluate the behavior of the filter element when installed into air filter assembly,
- Quantifying filter behavior with results of sector analyses and determining porous media tensor to represent filter element in complete AIS CFD model,
- Building a full CFD model including all low pressure portion of the AIS and evaluating flow performance in terms of pressure loss and flow characteristics such as flow uniformity values on before and after mass flow rate sensor, filter element and at compressor inlet.
- Gathering test results for the AIS subjected to CFD analyses and comparing pressure loss behavior to validate the evaluation method.
- Searching possibility to conduct the AIS evaluation process without requiring series of measurements.

1.2 Literature Review

Current methods employed in automotive industry are rather difficult to find since most of the information is kept as know-how inside automotive companies. However, with substantial amount of research on subject is known to be performed in numerous companies. These research methods mostly aimed to provide a reliable method to model AIS in terms of pressure losses and flow behavior.

In a SAE paper by Moreira et al. [3] 3D CFD analysis is performed for AIS of an automobile. In this analysis, filter element has planar and pleated geometry and modeled as a porous block. Analyses were conducted via commercial CFD solver FLUENT, and porous block's resistance parameters are obtained via series of tests on prototype, details of which are not shared.

Joshi et al. [4] worked on a methodology to evaluate low pressure ducts of a common rail direct injection engine. In this study the porous media coefficients of filter

elements that required by CFD solver is determined by a curve fit applied to the data obtained from series of tests conducted on an instrumented vehicle.

During literature survey for test-free methods for modelling filter element via CFD, a SAE paper by Huurdeman and Banzhaf [5] is encountered. The paper presents an application of the same main idea in this study. In this paper, the porous media coefficients are obtained with two-dimensional CFD modelling of single pleat in main flow direction. In other flow directions (by notation used in this thesis, against and parallel to pleats) simple flow analyses inside closed conduits are employed. Details of these analyses were not included inside the paper, due to preservation of know-how. The paper also contains an information for standard procedure of air filter design in Mann Hummel. Standard procedure is obtained by development of a tool by this company which generates pressure drop and porous media coefficients to be used in 3D CFD analyses upon user input of geometrical data and physical properties. Only study that provides information about CFD results' agreement with test for a model that includes air filter is provided by again Huuderman and Banzhaf (2006). In this study, level of agreement is found around 15%.

What these three studies share is to model the filter element as a porous block instead of solving the pleated filter geometry in full detail. Same simplification is used in this thesis due to its straightforward and yet reliable nature.

In most of the cases in literature, commercial CFD solvers such as StarCCM+, Fluent and CFX is employed to determine flow behavior. In a study by Siqueira et al. [6] an automobile AIS is analyzed for two different geometry configurations and seven different operation points for each geometry. Within this study it is found that the flow characteristics such as uniformity index (referred to as gamma coefficient) and eccentricity factor (a ratio that defines the location of maximum velocity with respect to axis of the section) is remaining unchanged with changing flow velocity.

In another study by Mamat et al. [7] pressure loss of air intake grill and duct located downstream is calculated. The study does not include filter element and all numerical results obtained is given in comparison with experimental data. CFD results show a maximum error of 8.4% from experimental data and authors deem this error level as fair level of agreement.

2. THEORY

2.1 Equations of Conservation

All equations of conservation including mass, momentum and energy is treated in integral form to comply with the necessity suggested by finite volume method (FVM). As defined by Andersson et al. [8], Finite Volume Method is based on dividing entire computational domain into small cells to represent partial differential equations (PDEs) that govern conservations of quantities as a sum of each cell's algebraic contribution. On this occasion, PDEs are reduced into a set of linear algebraic equations. These set of equations are given in the form that used in this study.

2.1.1 Continuity Equation (Conservation of Mass)

Continuity equation is the conservation of mass inside a domain whose boundaries are specified. In the analyses, unsteady effects are not taken into consideration. The continuity equation as provided in StarCCM+ v 10.02 theory guide [9]:

$$\oint_A \rho \vec{v}.\,d\vec{a} = \int_V S_u \, dV \qquad (2.1)$$

Where ρ is density, $\vec{v}$ denotes velocity vector and $\vec{a}$ is surface vector. S_u denotes the net mass generated inside volume element. $\oint_A$ is the symbol used to define a surface integral over a specified boundary.

2.1.2 Conservation of Momentum

Since the analyses are all solved buy steady solver, transient term is dropped to zero and all body forces acting on volume element is neglected except for porous media

force. After arrangements, the conservation equation for momentum is given by Equation (2.2) [9]:

$$\oint_A \rho \vec{v} \otimes \vec{v}.\,d\vec{a} = -\oint_A \rho I.\,d\vec{a} + \oint_A \tau.\,d\vec{a} + \int_V \overrightarrow{f_p}\,dV \qquad \textbf{(2.2)}$$

Left hand side of the equation is corresponding to convective flux; Where $\vec{v}$ is velocity vector, ρ is density $\vec{a}$ is the face area vector. The operator $\otimes$ used in equation is the tensor (dyadic) product of two vectors. Terms on the right hand side is corresponding to pressure gradient, viscous flux and body forces, respectively. And the variables $\rho, I, \tau, \overrightarrow{f_p}$ are corresponding to density, identity matric, viscous flux tensor and body force per volume caused by porous media involment, respectively. Since the Reynolds stress transport model is employed to solve cases as turbulent flow, Bousinessq approximation is used for viscous flux tensor τ [9]:

$$\tau = \mu_{eff}\left[\Delta\vec{v} + \nabla\overrightarrow{v^T} - \frac{2}{3}(\nabla.\vec{v})I\right] \qquad \textbf{(2.3)}$$

Inside Equation (2.3)., $\vec{v}$ is the velocity vector, $\overrightarrow{v^T}$ is the velocity vector defining turbulent fluctuations. $\mu_{eff} = \mu + \mu_{t\prime}$ is the effective viscosity and sum of the laminar viscosity μ and turbulent viscosity $\mu_{t\prime}$. Turbulent viscosity is defined as follows [8];

$$\mu_{t\prime} = \rho C_\mu \frac{k^2}{\varepsilon} \qquad \textbf{(2.4)}$$

In Equation (2.4), C_μ denotes realizable k-epsilon coefficient, k is turbulent kinetic energy and epsilon denotes turbulent dissipation rate.

In Equation (2.2), the variable $\overrightarrow{f_p}$ in body force addition term represents the effect of porous medium if CFD model includes a porous domain. The viscous body force term $\overrightarrow{f_p}$ is calculated by following formula as follows [9]:

$$\overrightarrow{f_p} = -(P_v + P_i|\vec{v}|).\vec{v} \qquad \textbf{(2.5)}$$

where P_v is porous viscous resistance and P_i denotes porous inertial resistance tensors. Determinationof these coefficients will be revisited in succeeding chapters.

2.1.3 Energy Equation (Conservation of Energy)

Energy equation used in analyses is for a flow, which is not transient and includes no body forces and grid velocity, and presented in integral form as follows [9]:

$$\oint_A \rho H \vec{v} d\vec{a} = -\oint_A \overrightarrow{q''} d\vec{a} + \oint_A \tau.\vec{v} d\vec{a} \tag{2.6}$$

where H is the total enthalpy $\overrightarrow{q''}$ is the heat flux vector τ is the viscous stress tensor that calculated in Equation (2.3), and $\vec{v}$ is the velocity vector. Total enthalphy H is calculated as;

$$H = h + \frac{|\vec{v}|^2}{2} \tag{2.7}$$

Heat flux vector $\dot{\overrightarrow{q''}}$ is evaluated from;

$$\dot{\overrightarrow{q''}} = -k_{eff} \nabla T \tag{2.8}$$

where T is temperature and k_{eff} is effective thermal conductivityk_{eff} is calculated as follows for porous media involvement:

$$k_{eff} = \chi k_{fluid} + (1 - \chi) k_{solid} \tag{2.9}$$

And χ is porosity (calculated from ratio of void volume over total volume) k_{fluid} is the effective thermal conductivity for turbulent flows:

$$k_{fluid} = k + \frac{\mu_{t'} C_p}{Pr_{t'}} \tag{2.10}$$

where k is thermal conductivity of the fluid, $\mu_{t'}$ is turbulent viscosity from Equation (2.4) C_p is specific heat, $Pr_{t'}$ is turbulent Prandtl number.

2.2 SIMPLE Algorithm

One of the most important aspects in CFD modelling is the coupling of velocity and pressure and pressure corrections applied in CFD model. The method called SIMPLE (Semi Implicit Method for Pressure Linked Equations) algorithm is employed by StarCCM+ solver to conduct this operations.

SIMPLE algorithm is an iterative process that starts from a guessed value (i.e. an initial condition prescribed by user for CFD solvers) for pressure field in domain subjected to CFD. SIMPLE algorithm includes following steps [9]:

1) Set the boundary conditions.

2) Computed the reconstruction gradients of velocity and pressure.

3) Compute the velocity and pressure gradients.

4) Solve the discretized momentum equation. This creates the intermediate velocity field $\vec{v}*$

5) Compute the uncorrected mass fluxes at faces $\dot{m}_f*$

6) Solve the pressure correction equation. This produces cell values for the pressure correction p'

7) Update the pressure field:

$$p^{n+1} = p^n + \omega p' \qquad (2.11)$$

where ω is the under-relaxation factor for pressure.

8) Update the boundary pressure corrections p'_b

9) Correct the face mass fluxes:

$$\dot{m}_f^{n+1} = \dot{m}_f* + \dot{m} \qquad (2.12)$$

10) Correct the cell velocities:

$$\vec{v}^{n+1} = \vec{v}* - \frac{V \nabla p'}{a'_p^v} \qquad (2.13)$$

10

Where $\nabla p'$ is the gradient of the pressure corrections a'^v_p is the vector of central coefficients for the discretized linear system representing the velocity equation, and V is the cell volume

11) Update density due to pressure changes.

12) Free all temporary storage.

2.3 Porous Media Modelling via CFD

Background theoretical information about flow in porous media is a large and complex topic with numerous aspects are needed to be taken into account. However, modelling inside CFD solvers does not differ much in nature. Since the CFD modelling is performed in StarCCM+ solver's theoretical guides is inspected throughly to obtain the exact formulation to be used. Effect of porous media to flow is modeled as a momentum sink [7].

Main mechanism of pressure and momentum loss is governed by Darcy's law. StarCCM+ employs Darcy's Law for small values of velocity as defined by Vafai [10]:

$$\nabla P = -\left(\frac{\mu}{\alpha}\right).v \tag{2.14}$$

where μ is dynamic viscosity, ∇P is pressure gradient, α is permeability coefficient and v is "Darcy Velocity" defined as ratio of volumetric flow rate over cross sectional area.

However, when turbulence is present, momentum and pressure drop behavior of region changes. Due to this change inertial resistance factor P_i is added to the momentum sink equation, presented in Equation (2.5).

In porous media modelling, in order to determine viscous and inertial resistance, flow velocity is related to pressure loss per unit length in a macroscopic manner as follows [9]:

$$\frac{\Delta P}{L} = P_v v + P_i v^2 \tag{2.15}$$

Equation (2.15) is the general form suggested for users to determine inertial and viscous resistance values. Generally, as can be seen in references [3] and [4], resistance values are calculated by fitting a polynomial to test data.

2.4 Finite Volume Method

There is a wide variety of numerical algorithms to solve these problems in literature, according to their position in mathematical classification. However, each algorithm requires an operation called discretization to solve the equation numerically. Zikanov [11] defines discretization as replacement of an exact, continuous solution of a PDE or a system of PDEs by an approximate numerical solution defined in a discrete domain. This replacement process can be performed in numerous ways including spectral, finite element, finite difference and finite volume methods. Commercial CFD solvers generally employ finite volume approach for solutions.

The FVM is a discretization technique for partial differential equations, especially those that arise from physical conservation laws. FVM uses a volume integral formulation of the problem with a finite partitioning set of volumes to discretize the equations. FVM is in common use for discretizing computational fluid dynamics equations. Detailed information for discretization of conservation equations can be found in the book in reference [8].

2.5 Computational Grid

Discretization of a computational domain requires representation of discretized quantity (geometry, time etc.) as set of points with known properties. This set of points form series of two or three dimensional elements. The structure formed by these elements is called "grid" or "mesh". Hoffmann and Chiang describes grids in two main categories; structured grid and unstructured grid. Sturctured grid is formed by elements rectangular in shape and grid points are distributed along the grid lines, whereas unstructured grid's points can not be associated with orderly defined grid lines, the points forming discrete elements are not distributed according to the same pattern throughout computational domain [11]. Figures 2.1 and 2.2 shows an example for structured grid and unstructured grid, respectively.
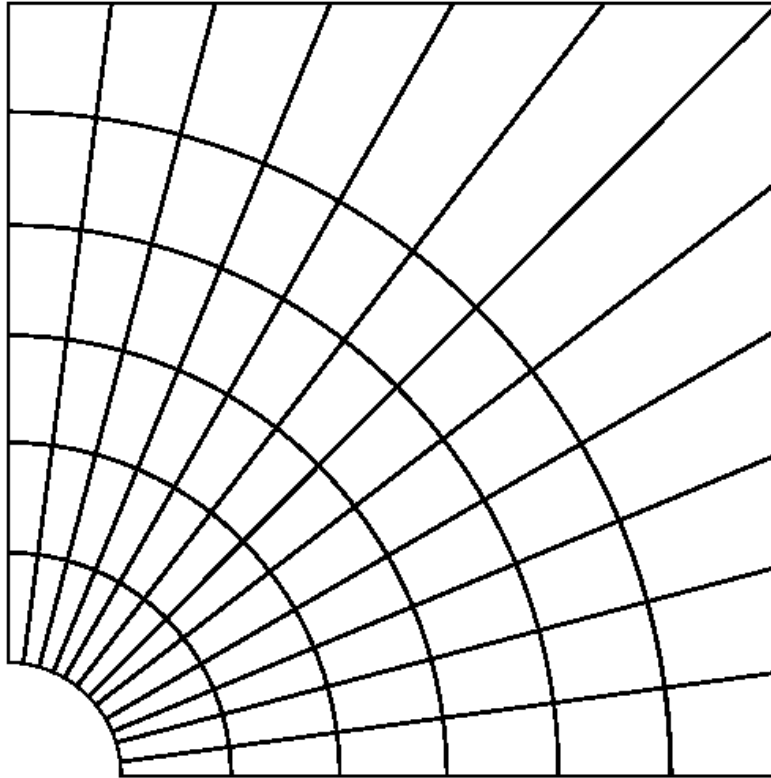
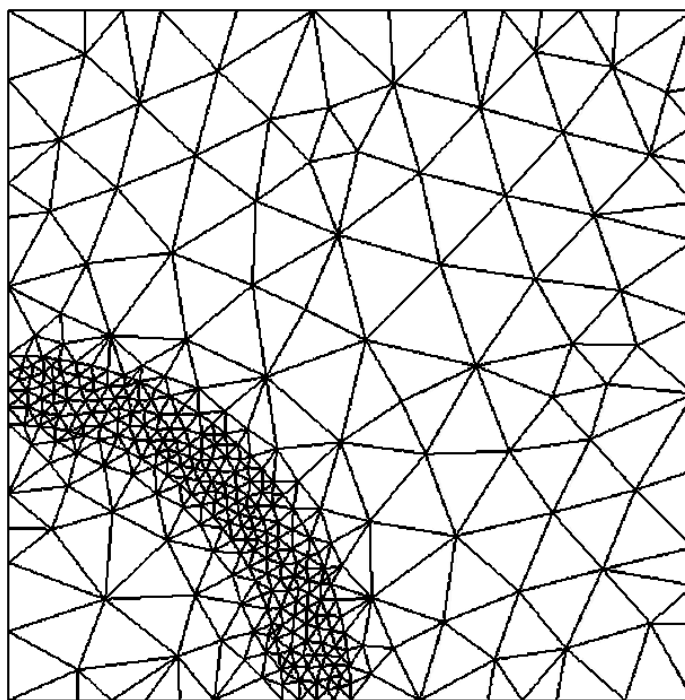**Figure 2.1 :** Structured grid, [12].

Figure 2.2 : Structured grid built with triangular elements.

CFD models built in this study also include unstructured mesh. Surface mesh generated to define basis for volume meshing used triangular element and volume mesh for all CFD models in this thesis is generated from polyhedral cells.

13

3. EVALUATION OF AIS

3.1 Workflow

In order to evaluate AIS, the all calculations are followed in a step by step manner. On this occasion, the whole workflow can be described in 4 steps. These steps are:

Step 1: Air Permeability Calculation of filter element:

- Geometry and other pertinent information is gathered for filter element to be used in next calculations.

- ASTM standard test procedure is applied on filter element or standardized filter permeability data is used to obtain permeability property of the filter element.

- A CFD model is built to evaluate the level of agreement between tests and CFD. In this CFD model, value of porous viscous resistance *Pi* is calculated from ASTM test and applied as isotropic porous media coefficient.

Step 2: Sector analyses:

- Mesh sensitivity study is performed for CFD models to be built up, to ensure optimized mesh quality and calculation time.

- A CFD model is prepared for each three main directions for filter element, described according to positioning with respect to filter pleat structures. The directions are named as parallel, perpendicular and against the pleats.

- CFD analyses for each direction is repeated to calculate porous inertial and viscous resistances. These coefficients are stored to be used in Step 3.

Step 3: Full geometry analysis:

- A CFD model is built for entire AIS, having a porous block instead of the filter geometry with all details.

- Mesh and runtime sensitivity study is performed.

- The coefficients for porous media obtained in Step2 are applied to this porous block.

- Upon completion of CFD analysis pressure and velocity contours in mass flow rate sensor, compressor inlet, upstream and downstream faces of porous filter element are provided.

- The pressure losses are calculated and reported for entire system and through filter element only.

Step 4 : System level validation test

- Test setup is build according to prescribed Ford procedure.

- The pressure readings on tests are collected and compared with the results obtained with CFD.

The workflow with sub elements is summarized with figure 3.1.
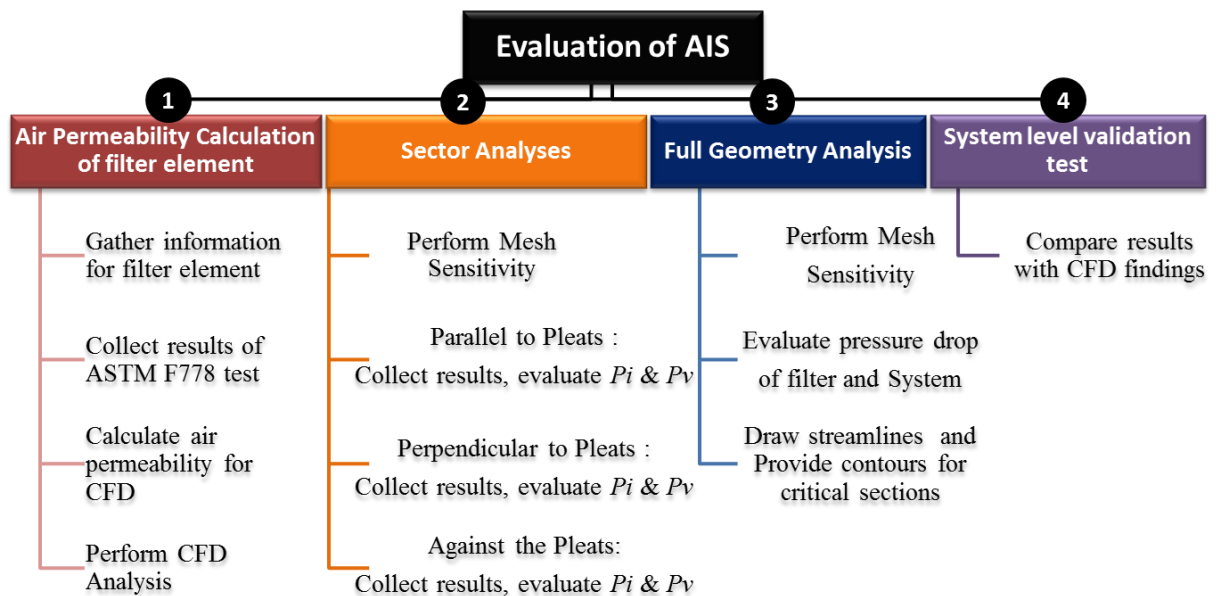
Figure 3.1 : Summarized workflow.

3.2 Step 1 : Air Permeability Calculation of filter element

3.2.1 Gathering information for filter element

To test and validate the method a sample case of analysis of an engine of which geometrical information and datasheets are provided by Ford Otosan is used. In the Figure 3.2 and table Table 3.1, the filter element's geometrical information is provided.
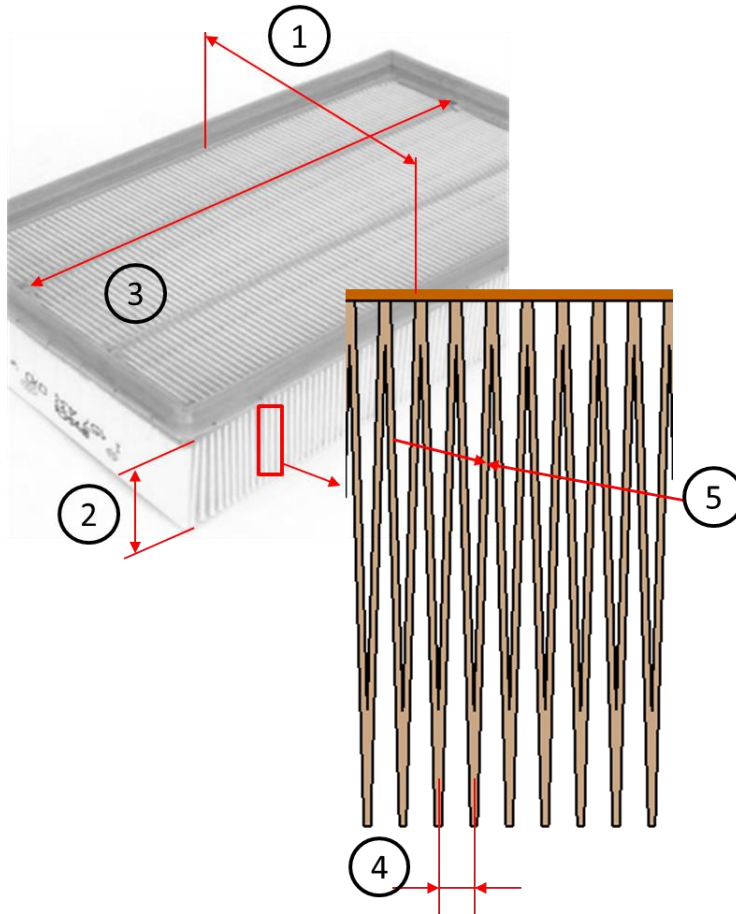
Figure 3.2 : Air Filter Geometry Details

As can be seen in Figure 3.2, due to its small details, modelling the filter element would pose extreme difficulties in both meshing and calculation phases for a full AIS geometry CFD study.

Table 3.1 : Geometry data for Filter Element [13]

Description	Dimension (mm)	Corresponding dimension on Figure 4.2
Number Of pleats	86	n/a
Bellow Width (mm)	168	1
Height of Bellow (mm)	45	2
Length of Bellow (mm)	266	3
Pitch of pleats	3.1	4
Thickness (mm)	0.5	5
Filtration Area (m2)	1.19	n/a

3.2.2 Gathering information for filter element

Most of the filter element producers comply with ASTM 738 standard test [13] to categorize their products. Filter element subjected to this study, Mahle LX935 air filter, is also categorized with aid of this test. According to standard test procedure, filter element used in assembly allows 440 l/min.m^2 of air flow from a 0.003532 m^2 of unfolded, circular filter element under 1 inch water column (124 Pa) pressure difference applied. Filter element is also known to have a thickness of 0.5 mm. This standard test result is used to calculate air permeability. And modifying this result, porous media coefficients to be used for sector CFD modelling of filter element is obtained. Darcy's law given in Equation (2.14) is employed to calculate air permeability.

Air permeability test is conducted for different filter elements to monitor repeatability, maximum deviation from test to test is below 2%. A schematic view of test setup is provided in Figure 3.3.
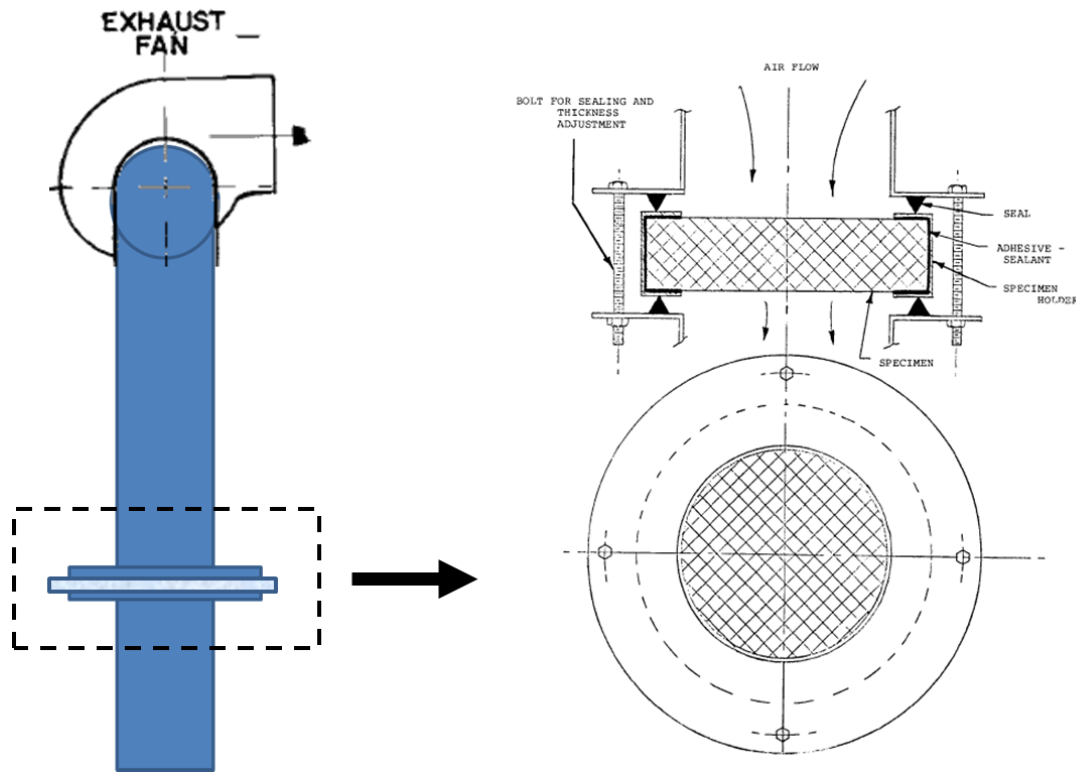
Figure 3.3 : Schematic Test Setup [13]

3.2.3 Calculate air permeability for CFD

During calculation of porous media coefficients, two main assumptions are employed. First, structure inside filter element assumed to be isotropic and show the same resistance in every direction. Second, flow inside the porous domain is assumed to be laminar and its behavior is governed by Darcy's Law. The porous viscous resistance P_v to be used in CFD model, is calculated from an altered version of Equation (2.14):

$$P_v = \frac{\mu}{\alpha} = \frac{vt}{\Delta P} = \frac{0.44(m/s)5x10^{-4}(m)}{124\ Pa} \cong 5.64x10^5 \left(\frac{kg}{m^3 s}\right) \tag{3.1}$$

where t is corresponding to filter element's thickness and ΔP is pressure drop across the filter element, v is superficial (Darcy) velocity and α is the air permeability coefficient of filter paper.

These values are used as isotropic tensor for "porous viscous resistance" for StarCCM+, value is fed to resistance coefficients matrix on CFD models in Step2, same value for all three directions.

3.2.4 CFD analysis

To perform the reliability crosscheck between test and CFD an analysis performed in accordance with geometrical specifications and requirements claimed in standard document. Model setup details are provided in tabular form via Table 3.2. In CFD model, total pipe length is set as 10 times the diameter of pipe to eliminate flow instabilities and to provide sufficient distance for flow to reach to the specimen without any resistance.

Boundary conditions for CFD model is extracted from ASTM test setup details.

- Inlet: Mass flow rate 2.06E-3 kg/s (cooresponds to 440 l/min.m^2 room temperature)

- Outlet : Pressure 0 Pa (Absolute)

It must also be noted that the specimen used inside the CFD model is assumed to be isotropic, that is to say, the specimen shows same porous media characteristic in all three dimensions.

Table 3.2 : CFD model setup data for Filter Element [14]

Quantity	Unit	Value
Filter Element Thickness	mm	0.5
Standard Cross Sectional Area	cm2	38.32
Density	kg/m3	1.22
Inlet Mass Flow	kg/s	2.06E-03
Pressure on outlet	pa	0
Deviation	N/A	7% <
Pressure Drop (Test)	Pa	124
Pressure Drop (CFD)	Pa	132

An image to show volume mesh is provided in Figure 3.4:
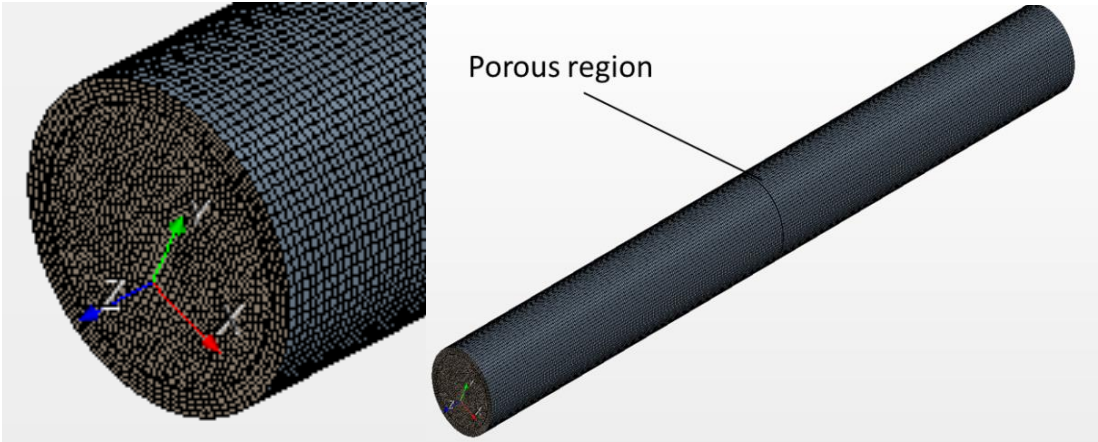
Figure 3.4 : CFD Model to mimic test conditions

The results obtained by CFD model is in good correlation with the prescribed pressure drop. The difference is calculated to be below 7%. In Figure 3.5, the CFD result is provided by a bar chart.
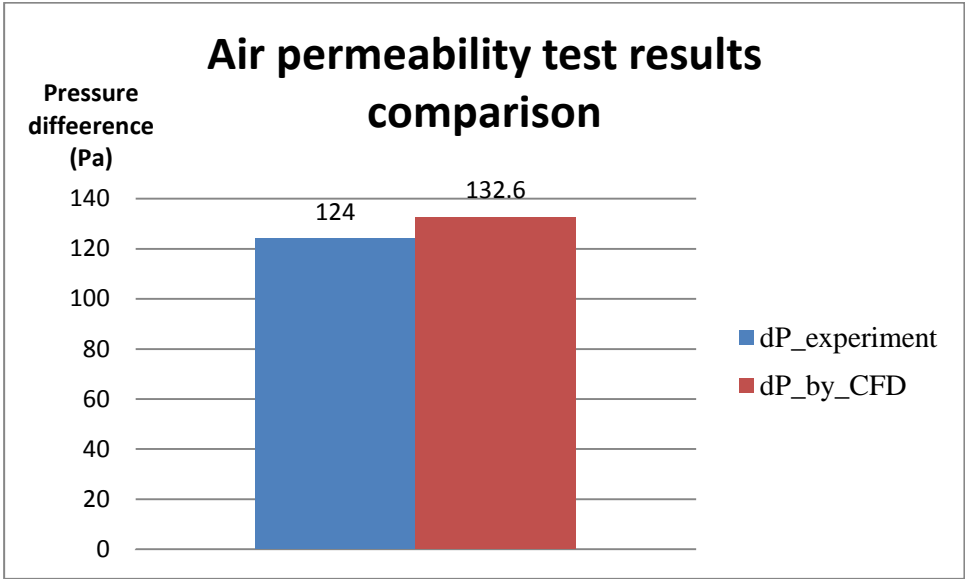

Figure 3.5 : ASTM F778 Test results and CFD model comparison

3.3 Step 2 : Sector Analyses

Sector modelling of air filter element is one of the most crucial parts of this study. A CFD model is prepared and performed for small portion of air filter element. Having a small portion enables modelling the geometry in full detail with considerably less penalty for runtime. Main problem is to recreate the domain in a representative way,

so that reliability of CFD results can hold. To accomplish this fidelity, structure is analysed in three main directions; parallel to pleats, perpendicular to pleats(main direction), and against the pleats. CFD models are run with mesh generated inside StarCCM+ having a range between 2.1 and 8.3 million polyhedral elements inside the domain. Mesh sensitivity study is performed with refinements until mesh independent solution is reached.

Three main flow directions are shown in Figure 3.6:
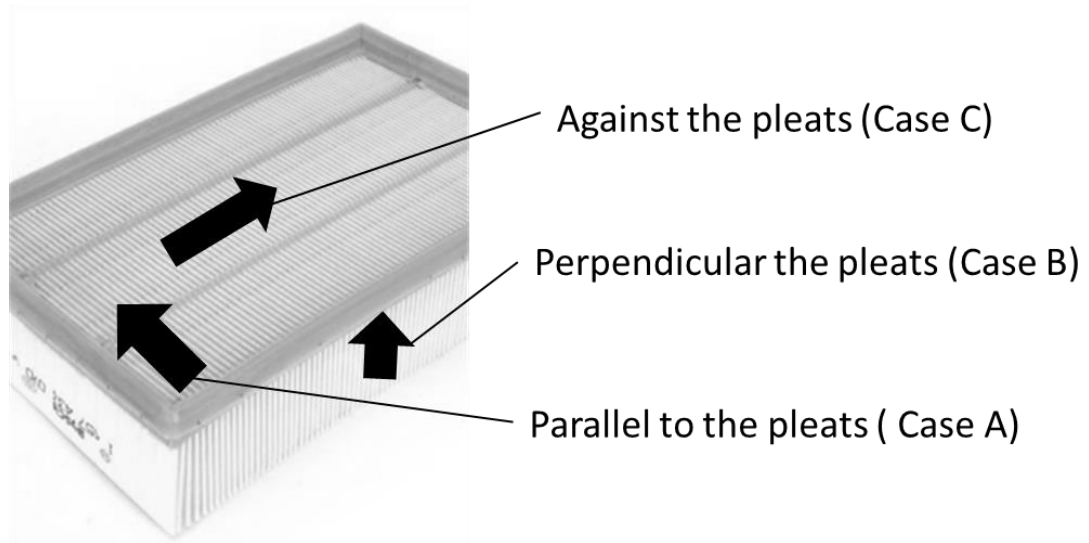
Figure 3.6 : Single Pleat analyses flow directions

Model setup details are divided into two groups as values and settings used in model and provided in tabular form as shown in table 3.3 and table 3.4 respectively.

Table 3.3 : Single Pleat (sector) analysis model setup details

	Quantity	Unit	Value
Mesh Values	Prism Layer Thickness	mm	0.1225
	# of Prism Layers	-	4
	Base Size	mm	0.3
	Absolute Minimum surface size	mm	0.03
	Absolute Target size	mm	0.2
	Surface Mesh Growth Rate	-	1.1
	Volumetric Control on corners mesh size	mm	0.03
Fluid Properties	Density	mm	1.205
	Viscosity	Pa.s	1.82E-05
	Thermal Conductivity	W/m-K	0.02603
	Specific Heat	J/kg-K	1005
Initial Conditions	Pressure	Pa	0
	Static Temperature	C	25
	Turbulent Lengthscale	mm	0.0463
	Turbulent intensity	-	0.05
	Porous side turbulence intensity	-	0.05
Boundary Conditions	Outlet Pressure	Pa	0
	Outlet Temperature	C	25
	Outlet Turbulent Lengthscale	mm	0.0463
	Outlet Turbulence Intensity	-	0.05
	Inlet Velocity	m/s	0.02-12
	Inlet Temperature	C	25
	Inlet Turbulent Lengthscale	mm	0.0463
	Inlet Turbulence Intensity	-	0.05
	Porous viscous Resistance (xx direction)	kg/m^3-s	590476.2
	Porous viscous Resistance (yy direction)	kg/m^3-s	590476.2
	Porous viscous Resistance (zz direction)	kg/m^3-s	590476.2
	Porous Inertial Resistance (xx direction)	kg/m^4	0
	Porous Inertial Resistance (yy direction)	kg/m^4	0
	Porous Inertial Resistance (zz direction)	kg/m^4	0

Table 3.4 : Single Pleat (sector) analysis physics setup details

Mesh Count	2.1M - 3.5 M
Turbulence Model	RANS > Realizable K-Epsilon Two Layer
Wall Treatment	All y+
Y+ Range	<1
Density Dependency	Ideal Gas
Time Dependency	Steady State
Temperature Dependency	Segregated

3.3.1 Mesh sensitivity analyses:

A mesh sensitivity study is performed to set the optimum mesh count for a both computationally economic and mesh independent solution. Only changed parameter during mesh sensitivity study is the base size.

Mesh sensitivity study is conducted for Case-A, has the flow in direction parallel to the pleats. To obtain mesh independent solution, three base size values are used:

- Coarse (includes 5.0E+5 Elements),

- Fine (includes 2.1E+6 elements),

- Very Fine(includes 2.6E+6 elements).

To demonstrate mesh density, Figure 3.7is provided. Each section view is extracted from same location, from the area marked in the Figure 3.7.
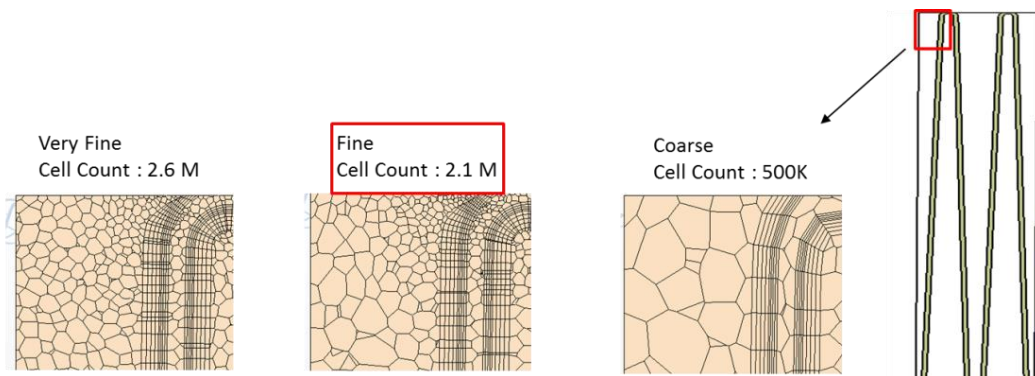
Figure 3.7 : Mesh sensitivity study images

Results provided in Table 3.5 and Figure 3.8.

Table 3.5 : Tabular data for sector analysis

	COARSE		FINE		VERY FINE	
Velocity(m/s)	ΔP (Pa)	ΔP/L(Pa/m)	ΔP (Pa)	ΔP/L(Pa/m)	ΔP (Pa)	ΔP/L(Pa/m)
0.2	1.225	245.00	1.065	212.97	1.198	239.55
0.4	1.698	339.66	1.711	342.24	1.860	371.99
0.6	2.516	503.15	2.621	524.11	2.654	530.71
0.8	3.402	680.41	3.567	713.41	3.558	711.66
1	4.334	866.85	4.542	908.37	4.514	902.70
1.2	5.310	1062.03	5.543	1108.56	5.502	1100.41
# of cells	500 000		2 100 000		2 600 000	
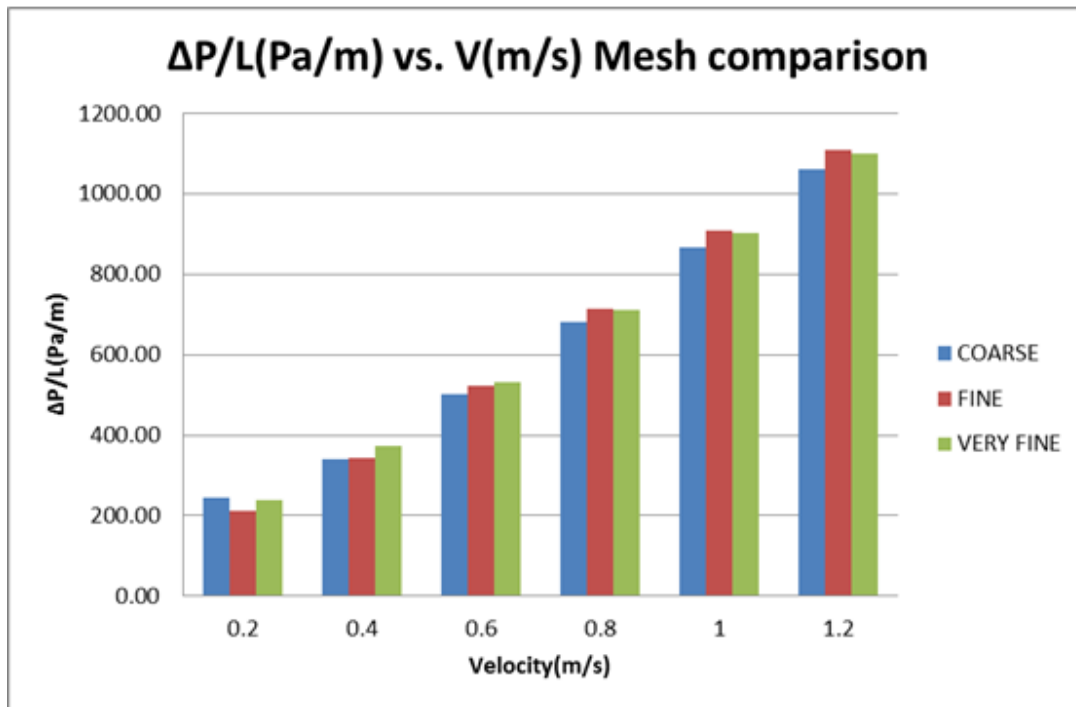
Figure 3.8 : Mesh sensitivity study results

Method was to make the mesh finer and finer until mesh independent results are obtained. Since the pressure drop values differ less than %3, case called 'Fine' is chosen.

3.3.2 Case A: Parallel to pleats

Once the mesh size is determined, the procedure proceeded to sector analyses. The first analysis performed is called Case A. Geometry details for Case A is given with Figure 3.9 and 3.10.
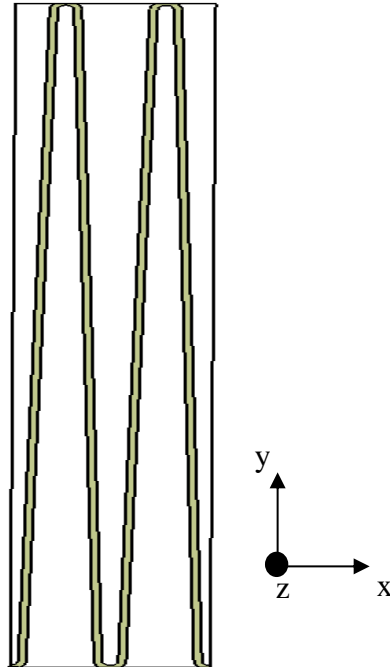
Figure 3.9 : CFD domain for parallel to the pleats case
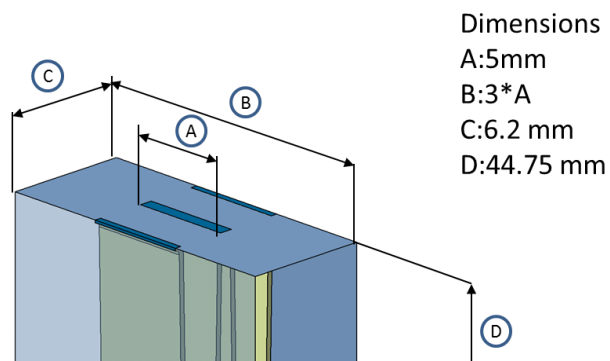
Figure 3.10 : Geometrical dimensions for case A

Figure 3.11 provides images of CFD domain from different angles and computational grid.
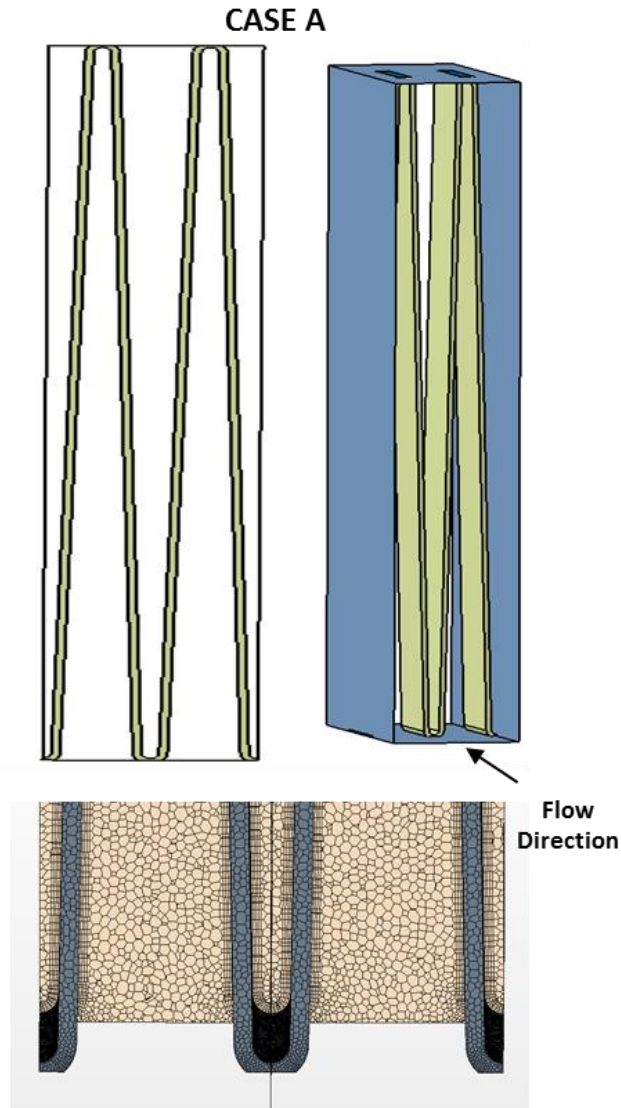
Figure 3.11 : CFD domain for case A

In this model, sketch shown in Figure 3.9 is created in CATIA, extruded in direction perpendicular to the sketch plane namely the z direction, and exported to StarCCM+. Flow in this case is through the pleats, in z direction. Pleats are modeled as isotropic porous media. Boundary conditions for CFD model:

- Inlet: Velocity Inlet, 0.2-1.2 m/s (swept with 0.2 intervals)

- Outlet: Pressue Outlet 0 Pa (gage).

It must be noted that velocity values are extents of typical values expected under real operating conditions for given direction.

Upon completion of analyses, the pressure loss data is obtained as shownin table 3.6.

Table 3.6 : Tabular Input/Output Data for CFD Analyses

StarCCM+	
V	ΔP(Pa)
0.20	1.07
0.40	1.71
0.60	2.63
0.80	3.58
1.00	4.56
1.20	5.56

To extract porous media coefficients, ΔP is normalized with characteristic length of porous media, namely the depth of pleat structure. For the depth value of 5mm, normalized pressure values plotted with corresponding velocity values, creating the characteristic curve for porous media coefficients extraction.
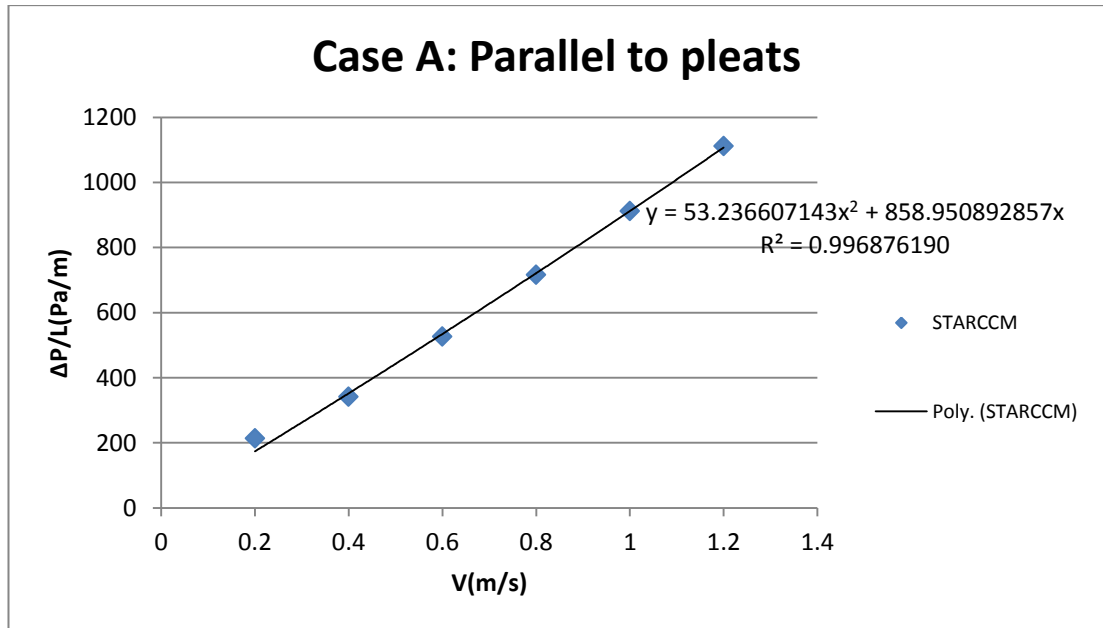
Figure 3.12 : Polynomial curve fit for Case A

With fitted curves, polynomial coefficients can be directly used as porous inertial and viscous coefficients inside StarCCM+ model. Tabular data from Table 3.6 with calculated porous inertial and viscous resistances are provided in Table 3.7.

Table 3.7 : Pressure loss characteristics and porous media coefficients

V(m/s)	STARCCM ΔP/L(Pa/m)
0.20	213.25
0.40	342.95
0.60	525.46
0.80	715.38
1.00	911.01
1.20	1111.94
Porous inertial Resistance	53.49
Porous Viscous Resistance	858.25

Pressure and velocity contours provided for given section indicated in the figure 3.13.
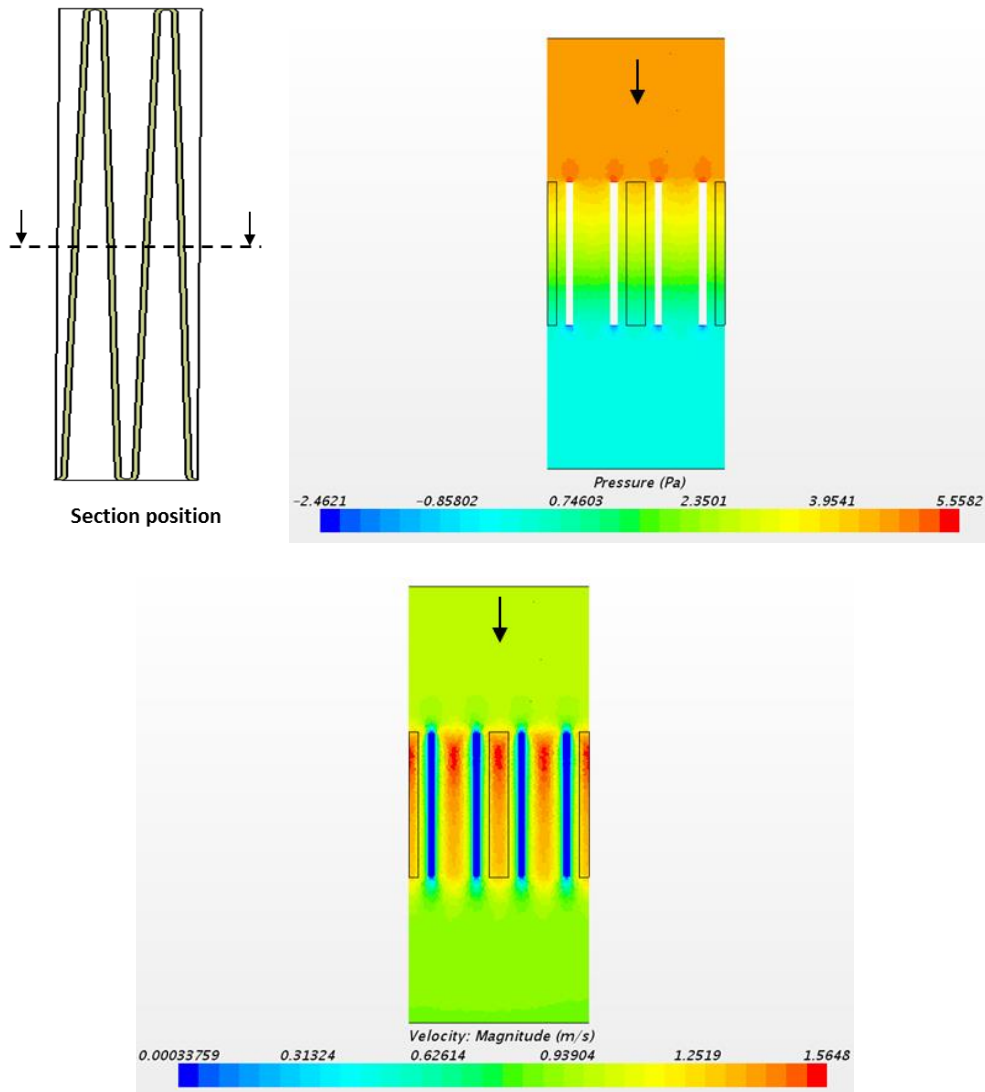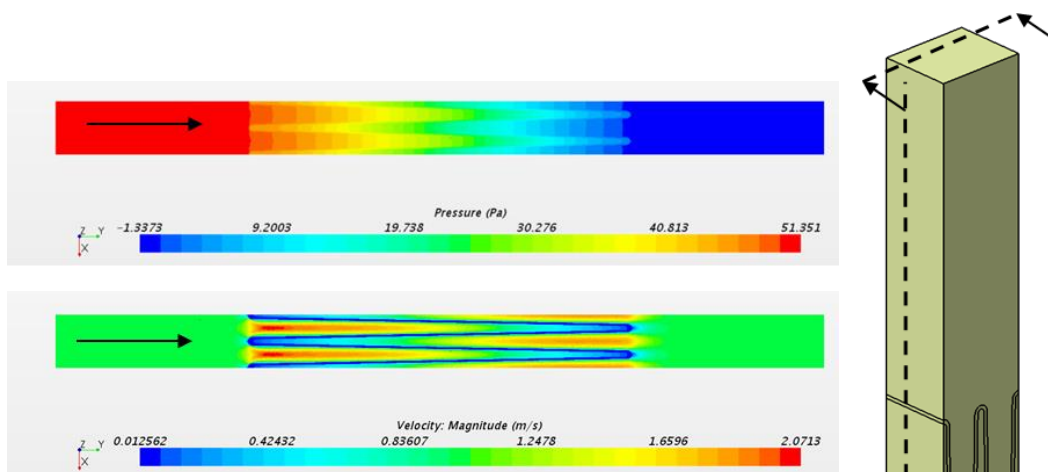

Figure 3.13 : Pressure and velocity contours for case A

3.3.3 Case B: Perpendicular to pleats
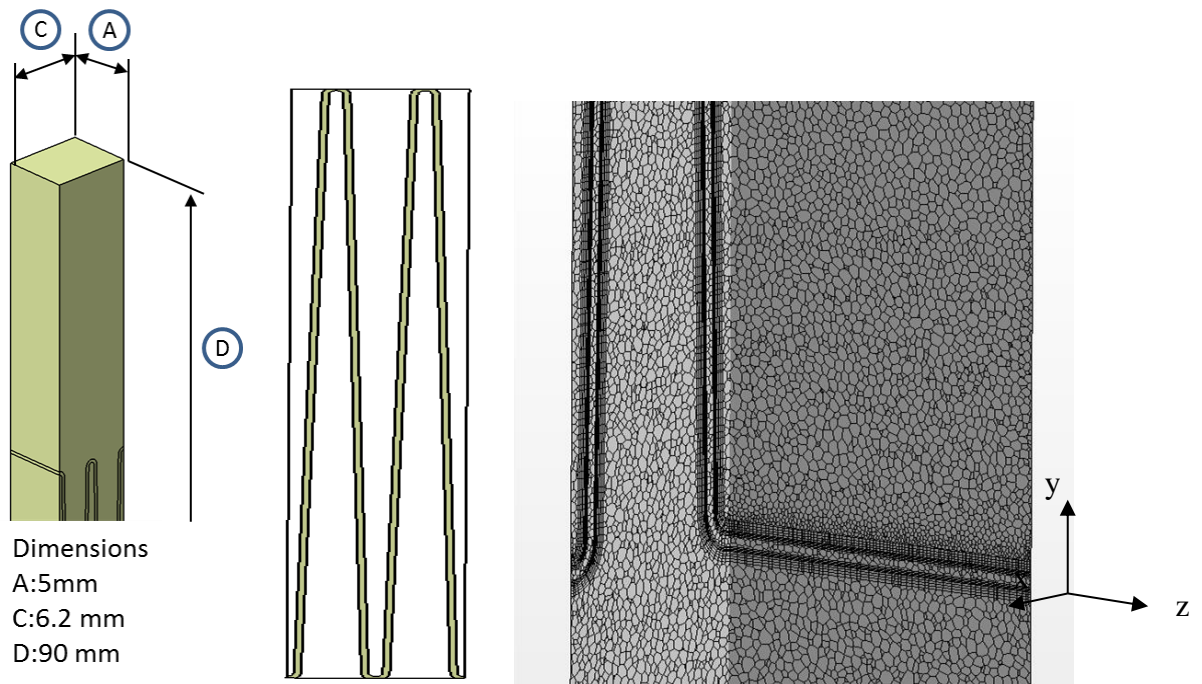
Figure 3.14 : CFD domain for perpendicular to the pleats case and sample grid

In this model, sketch shown in Figure 3.14 is created in CATIA, extruded in direction perpendicular to the sketch plane, namely the z direction, and exported to StarCCM+. Flow in this case is through the pleats, in -y direction. Pleats are modeled again as isotropic porous media. Boundary conditions for CFD domain are:

- Inlet : Velocity Inlet: 2-12 m/s (swept through with 2 m/s intervals).

- Outlet : Pressure Outlet, 0 Pa (gage)

Velocity values are extents of typical values expected under real operating conditions for given direction.

To extract porous media coefficients, ΔP is normalized with characteristic length of porous media, namely the height of pleat structure. For the normalized pressure values plotted with corresponding velocity values, creating the characteristic curve for porous media coefficients extraction. Characteristic curves and porous media coefficients are shared in Figure 3.15 and Table 3.8, respectively.
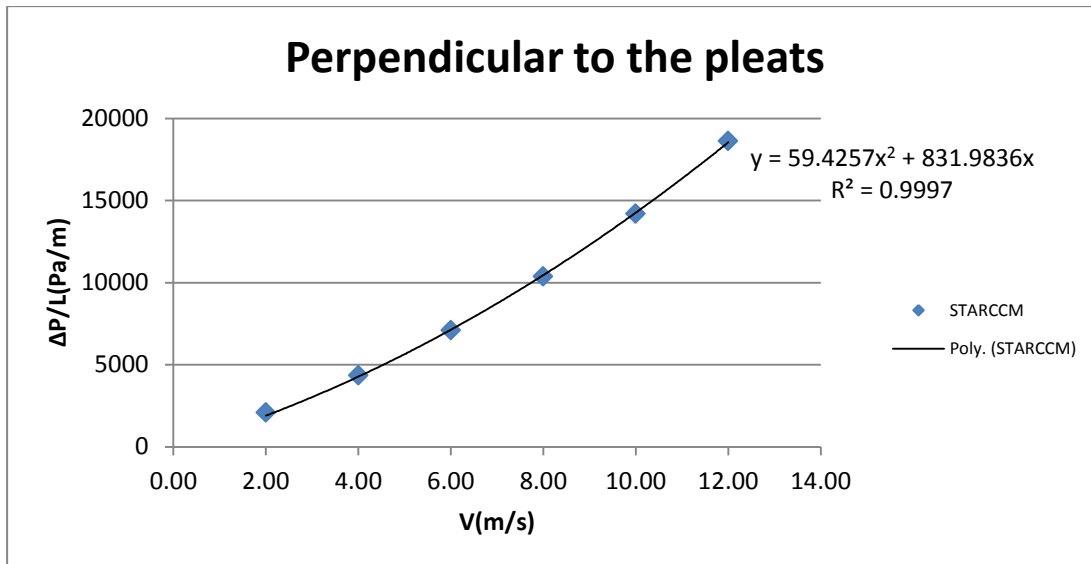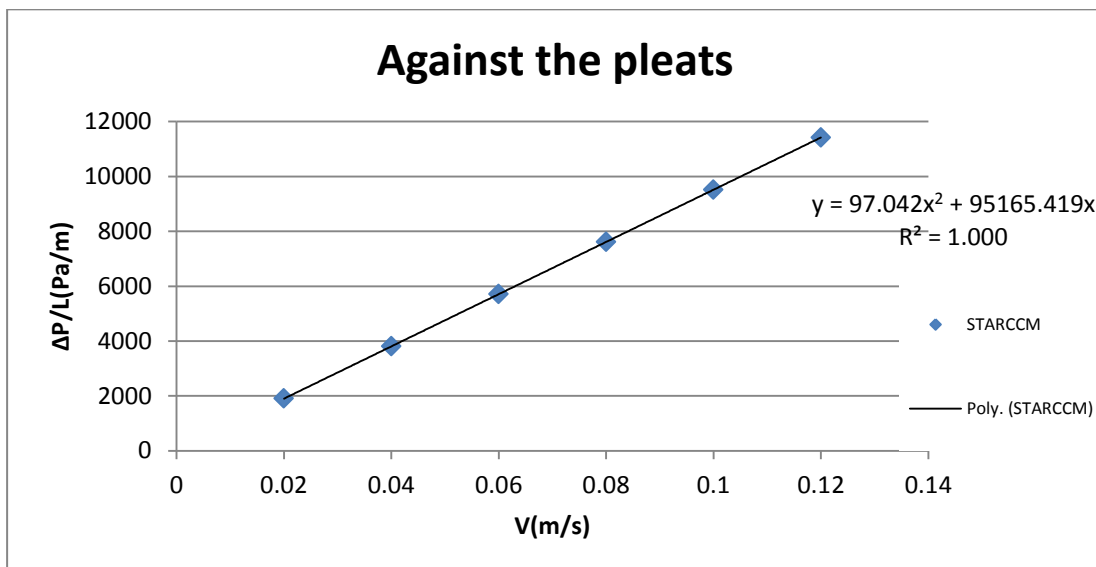
Figure 3.15 : Polynomial curve fit for Case B

Table 3.8 : Pressure loss characteristics and porous media coefficients

	STARCCM
V(m/s)	$\Delta P/L(Pa/m)$
2.00	2084.01
4.00	4344.32
6.00	7088.25
8.00	10364.81
10.00	14203.39
12.00	18622.40
Porous inertial Resistance	59.43
Porous Viscous Resistance	831.98

Pressure and velocity contours provided for given section indicated in the Figure 3.16.

Figure 3.16 : Position of the plane section and Pressure & Velocity Contours

3.3.4 Case C: Against thepleats
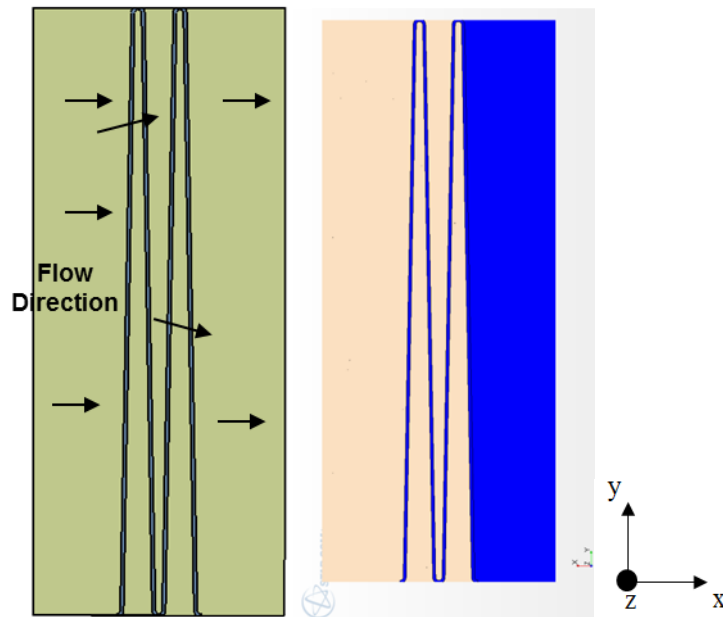
Figure 3.17 : CFD domain for against the pleats case

Dimensions
A:5 mm
C:6.2 mm
D:44.75 mm
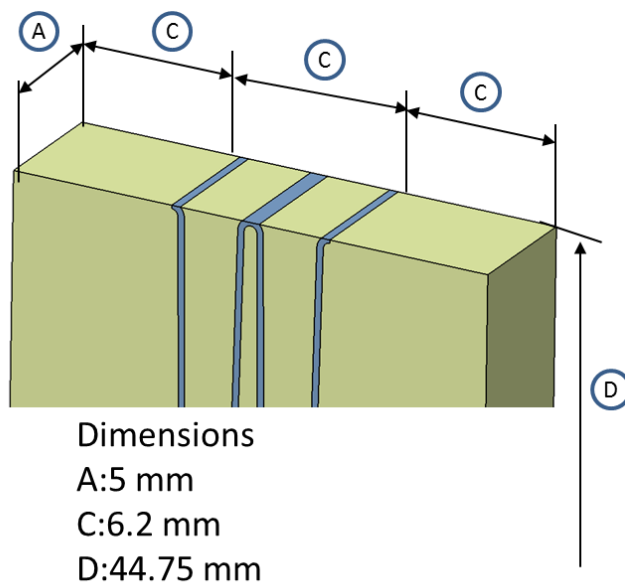
Figure 3.18 : Geometrical dimensions for case C

In this model, flow in this case is through the pleats in x direction as shown in Figure 3.17. CFD Model is prepared according to geometry infromation provided in Figure 3.18. Pleats are modeled again as isotropic porous media. BOundary conditions for CFD Analyses are:

- Inlet : Velocity Inlet 0.02-0.12 m/s (swept through with 0.02 m/s intervals).

- Outlet : Pressure Outlet, 0 Pa (gage)

Velocity is swept through 0.02-0.12 m/s with 0.02 m/s intervals. Velocity values are extents of typical values expected under real operating conditions for given direction.

To extract porous media coefficients, ΔP is normalized with characteristic length, namely the longest distance enveloped by region in x direction, For the normalized pressure values plotted with corresponding velocity values, creating the characteristic curve for porous media coefficients extraction. Characteristic curves and porous media coefficients are presented in Figure 3.19 and Table 3.9, respectively.

Figure 3.19 : Polynomial curve fit for Case C

Table 3.9 : Pressure loss characteristics and porous media coefficients

	STARCCM
V(m/s)	ΔP/L(Pa/m)
0.02	1903.64
0.04	3806.45
0.06	5709.68
0.08	7614.52
0.10	9517.74
0.12	11420.97
Porous inertial Resistance	97.21
Porous Viscous Resistance	95165.39

3.4 Step 3 : System Level CFD Analysis

Low pressure ducts refer to series of air channels and vessels conducting air from free atmosphere to compressor. A typical low-pressure AIS ducts consists of following parts; snorkel, dirtyside duct, air filter box upstream, air filter element, air filter box downstream, cleanside duct. Main goal of this study is to obtain coefficients of porous block that represents the air filter element and use the values to model an AIS comprising the filter element . To do so, at this step of the method, obtained values of porous media is fed to the general model. The model contains 3 different regions, namely Fluid region for upstream, a porous region representing the filter element and another fluid region to solve downstream.

CFD analysis is performed via StarCCM+(v10.02). Wet surfaces extracted in CATIAV5R18, porous region modeled as a rectangular prism box and coefficients of porous media is defined as non-isotropic tensor including two terms, namely porous inertial resistance and porous viscous resistance retrieved from tables 3.7, 3.8 and 3.9. These values are applied to CFD model after defining a reference coordinate system in accordance with filter geometry.

3.4.1 Mesh Sensitivity Study

A mesh sensitivity study is performed to set the optimum mesh count for a both computationally economic and mesh independent solution. Only changed parameter during mesh sensitivity study is size of the mesh, size of the mesh and polyhedral cell growth rate.

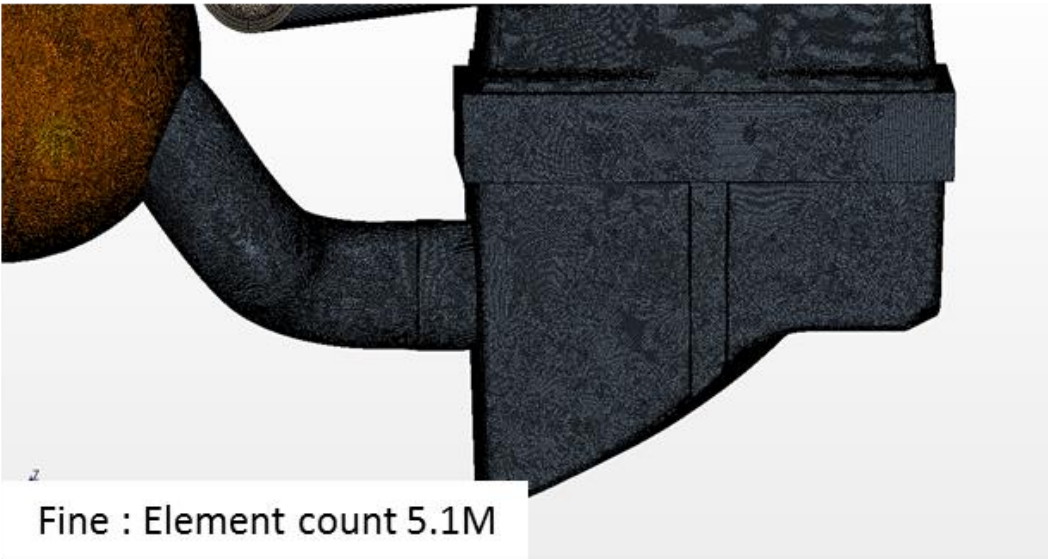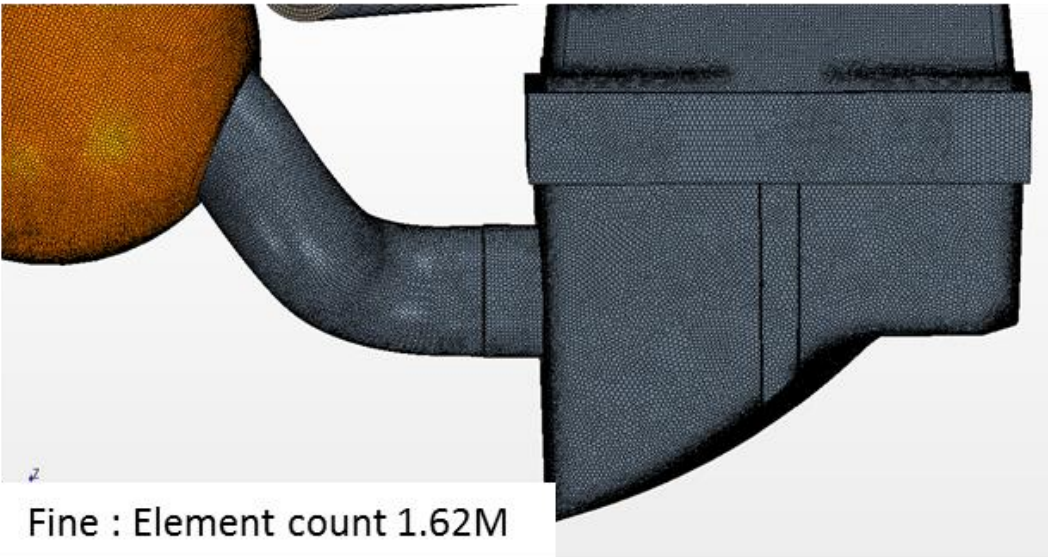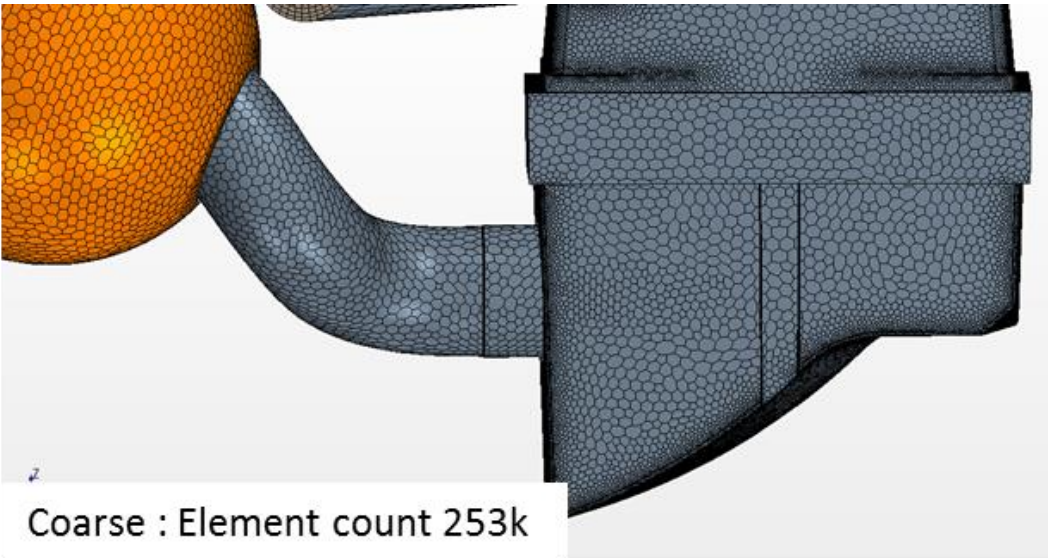Figure 3.20 shows the mesh density from left side view of the airbox geometry.

Coarse : Element count 253k

Fine : Element count 1.62M

Fine : Element count 5.1M

Figure 3.20 : Mesh sensitivity images for main model

Upon completion of the analyses, two metrics are compared for each model, namely; surface uniformity index at filter outlet and pressure loss throughout the system. Criterion for the study is that these metrics for "fine" model should not deviate more than 2% from "very fine" case. Method is built in such a way that if this deviation exceeds 2%, "Very fine" case become "fine" and new "very fine" case has increased mesh density. In this study target of 2% is attained within first trial.

The deviation of both metrics are provided in bar chart form with Figure 3.21 and Figure 3.22.

Surface Uniformity @ Filter outlet % Deviation (wrt Very Fine)
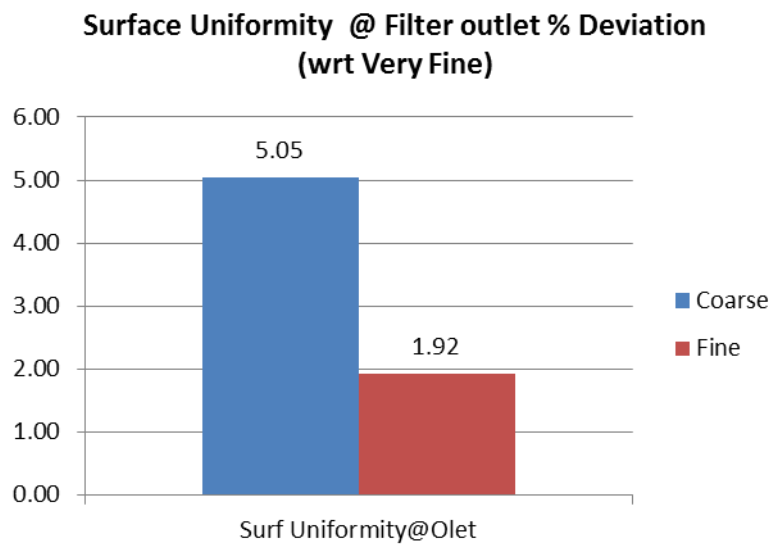
Figure 3.21 : Deviation of surface uniformity index calculated at filter outlet

Pressure Drop % Deviation (wrt Very Fine)
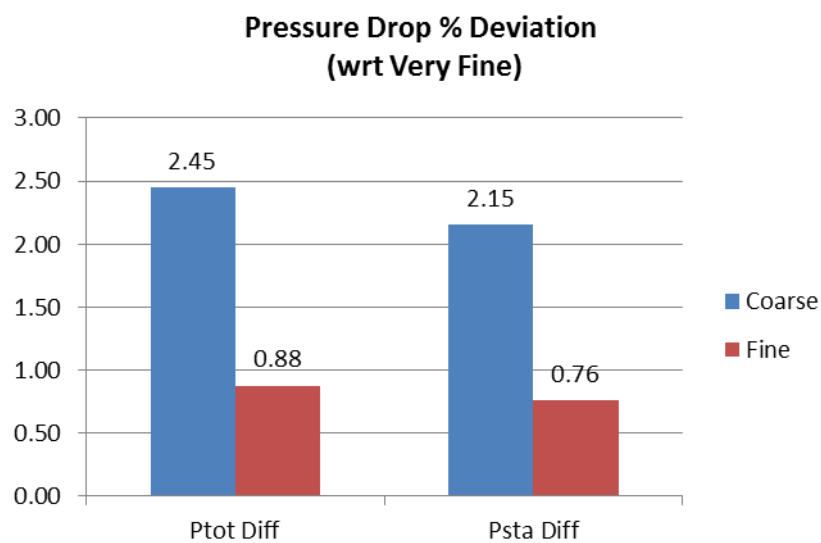
Figure 3.22 : Deviation of pressure drop calculated for entire domain

3.4.2 Pressure drop evaluation for AIS and filter element

As mentioned in the introduction section, in order to evaluate an automotive air intake system's flow characteristics, the analyses should be performed in two steps. First step includes detailed modelling of the filter element. This modelling provides necessary data for determination of porous media coefficients. These coefficients are then fed to porous media settings inside main model.

AIS CFD model consists of an intake tube (cleanside duct), Airbox, resonator and filter assembly, a cleanside duct and a representative mass flow rate sensor mounted on cleanside duct. Air is collected from fictionally defined spherical region to represent pressure losses that occur during suction of stationary, ambient air. Ambient pressure is applied as inlet boundary condition on surface of said fictious sphere. To provide desired mass flow through system, mass flow boundary condition is applied to the outlet side. Amount of mass prescribed at outlet is equal to mass flow rate for the condition that engine is running with rated power. High y+ turbulence model employed as wall treatment model, with a prism layer mesh configuration satisfying y+>30 condition for non-stagnant regions. Realizable k-epsilon turbulence model is used to simulate turbulent effects. During meshing, a fictional extrusion of 5 times outlet diameter is applied to the outlet boundary, to disregard the outlet effects and prevent numerical errors. However, pressure value at outlet is read from original location.

Model basically includes three regions namely cleanside ducts, porous block, dirtyside ducts as shown in figure 3.23.
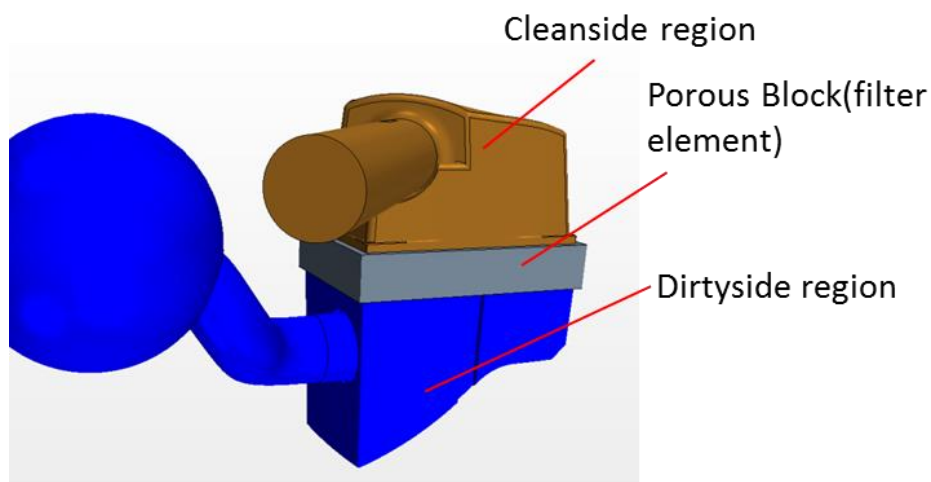

Figure 3.23 : Regions used in main CFD model

A fictious sphere is defined at the inlet to simulate suction from stagnant air and take the losses occur during suction into account. Inlet sphere is defined to be 5 times inlet pipe diameter. The figure 3.24 shows the fictious sphere.
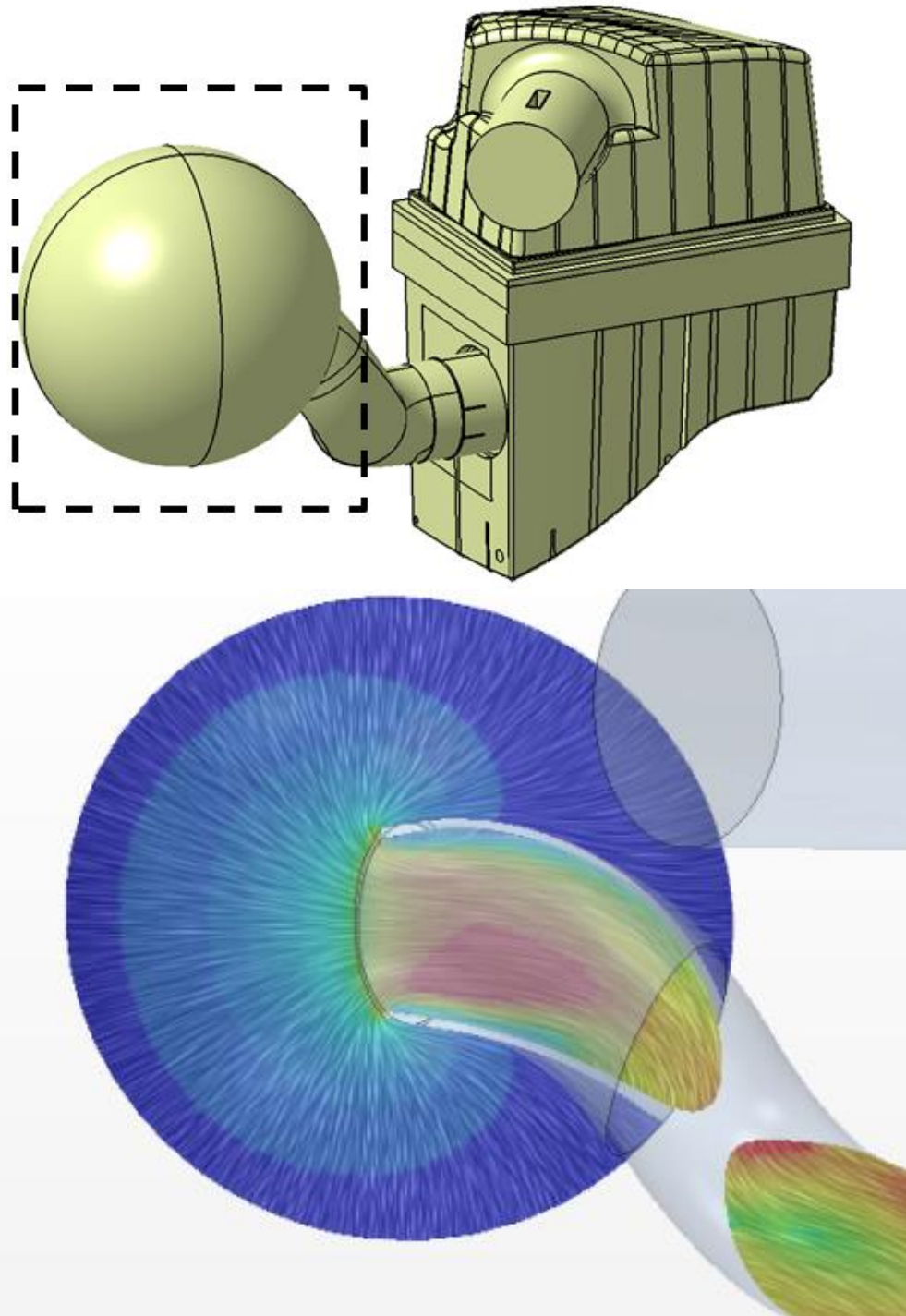

Figure 3.24 : Fictious sphere applied on inlet

The most important output of the study is without doubt, the pressure drop value of systrm and its distribution among the components. To show the breakdown of pressure losses, a number of sections are provided within CFD model. Locations of these sections are marked in the Figure 3.25.
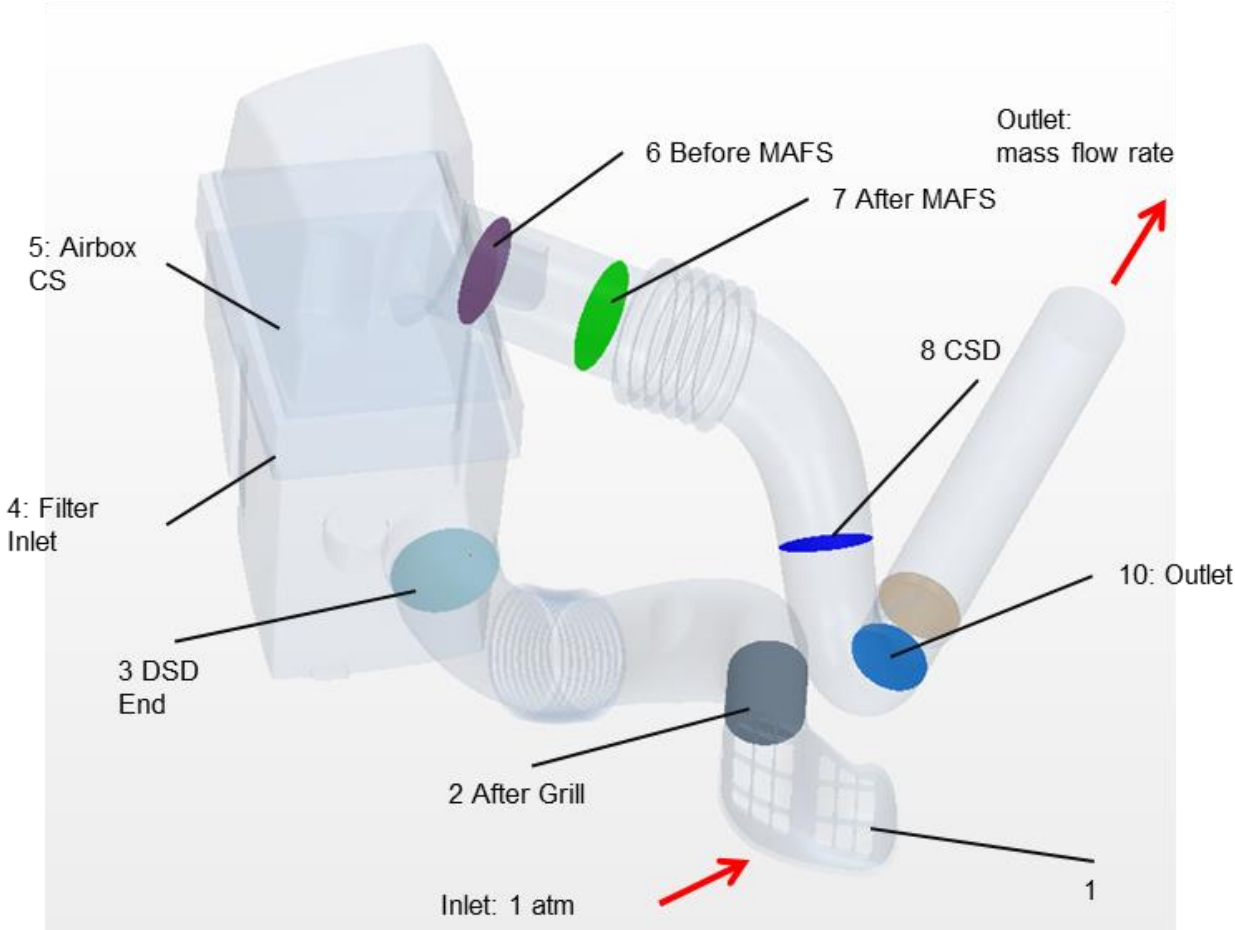
Figure 3.25 : Critical sections that CFD data is read

Pressure losses are normalized and provided as a percentage of total pressure loss throughout the system. Table 3.10 shows the pressure loss data where Figure 3.26 shows losses graphically via a bar chart.

Table 3.10 : Normalized Pressure Loss data

	ΔP Scaled to total ΔP level of system	
	CFD Results	
	Elementary	Cumulative
Inlet	0	0.00
Grill	28.7	32.25
Dirtyside Duct	17.7	52.13
Airbox Downstream	21.52	76.31
Filter	**11.08**	**88.76**
Airbox Upstream	1.33	90.26
Cleanside Duct	11.67	100.00
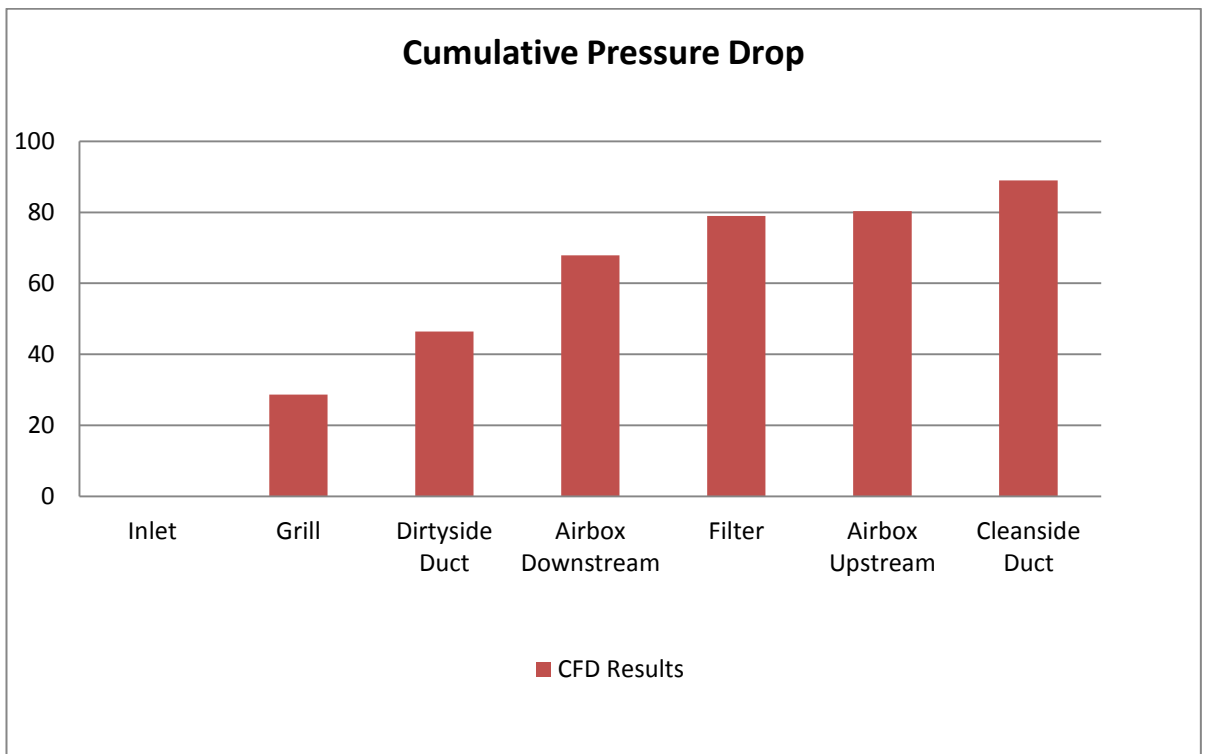
Figure 3.26 : Cumulative pressure loss data for components

3.4.3 Generation of streamlines and contours for critical sections

Upon completion of the analyses, pressure and velocity contours on streamlines and middle sections are provided. Figure 5.27 shows the position of section
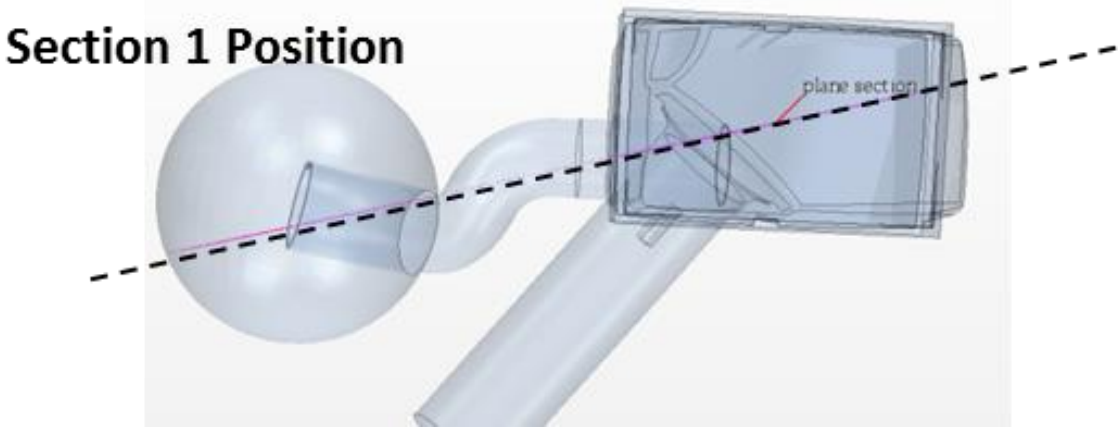
Figure 3.27 : Position of section 1

Velocity and Pressure contours on Section1 are provided in the figure 3.28 and 3.29:
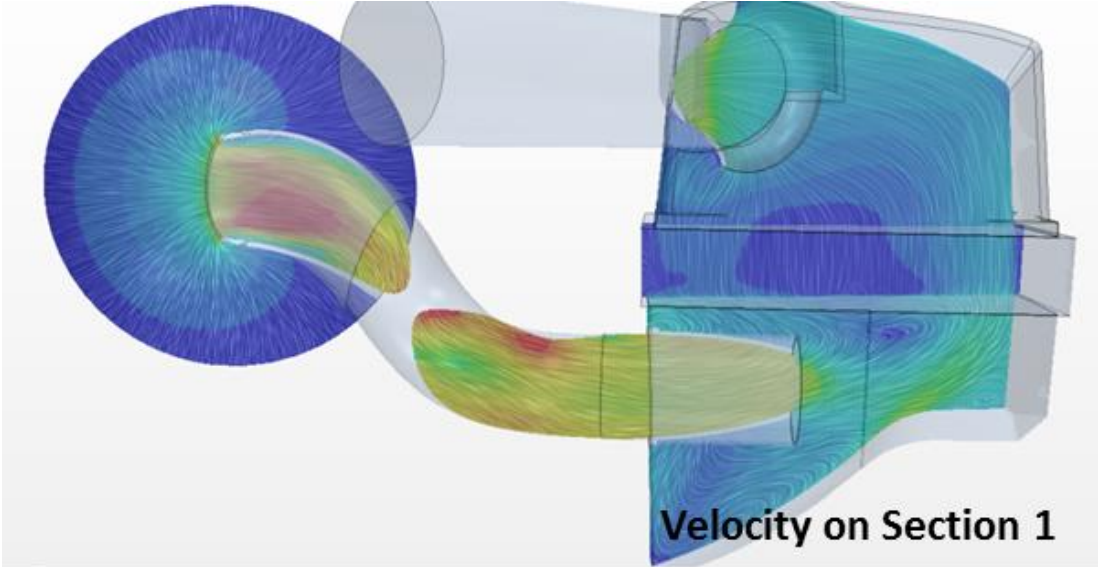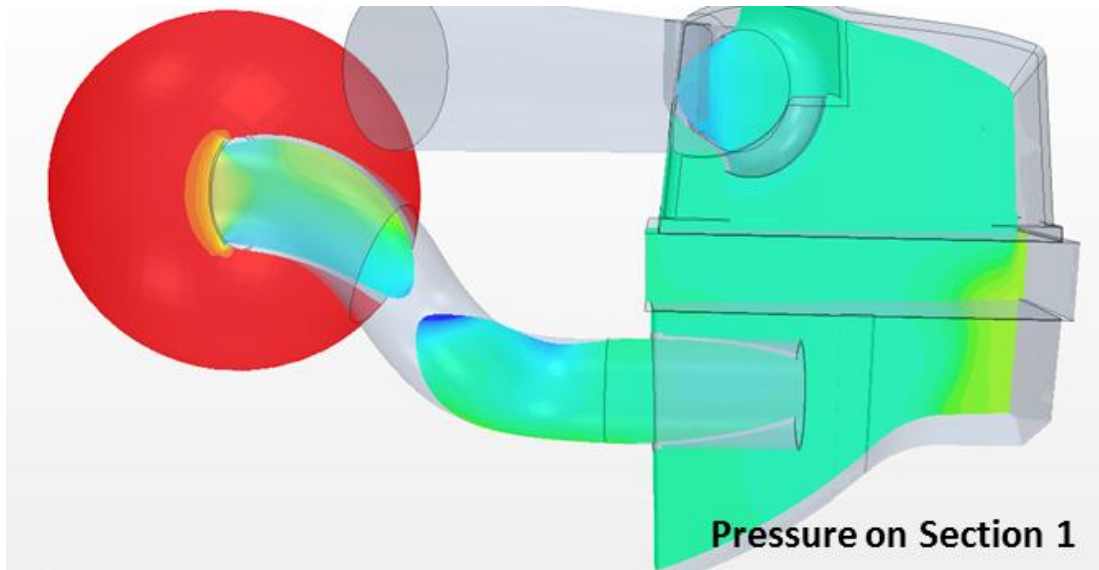

Figure 3.28 : Velocity and Pressure contours

Pressure on Section 1

Figure 3.29 : Velocity and Pressure contours

Streamline plots having pressure and velocity contours are provided in Figure 3.30 and figure 3.31:

Velocity Streamline
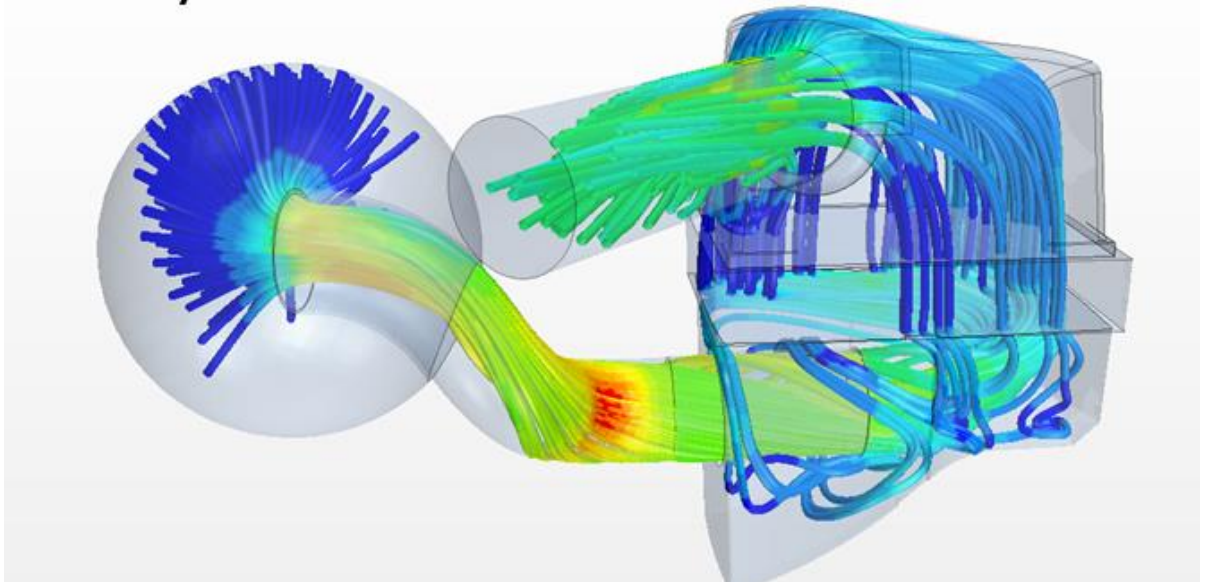
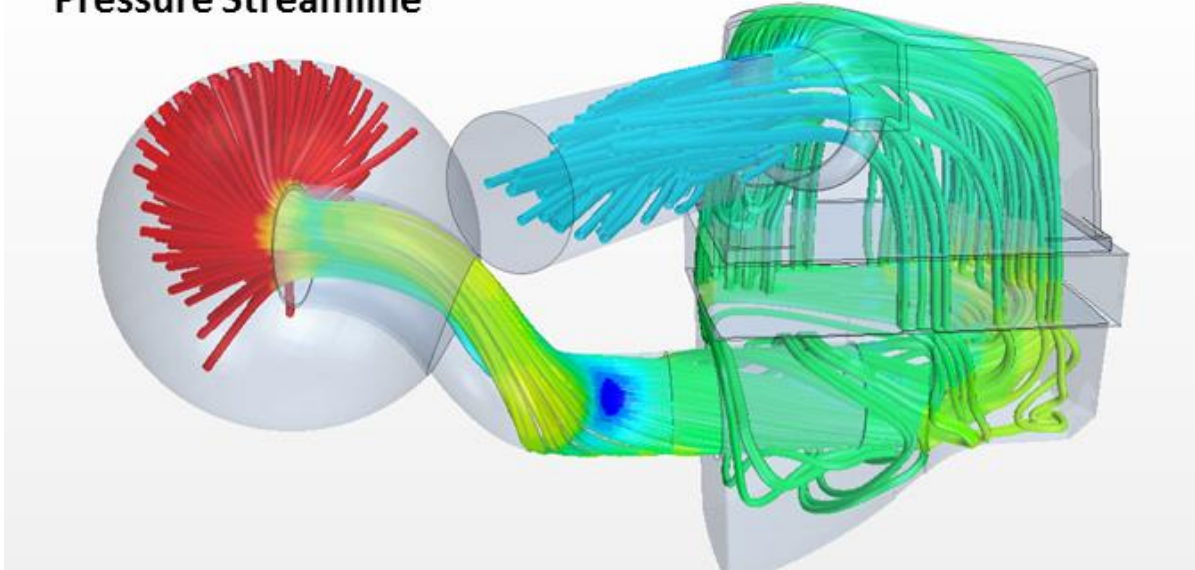**Figure 3.30 :** Velocity and Pressure contours

Figure 3.31 : Velocity and Pressure streamline plots

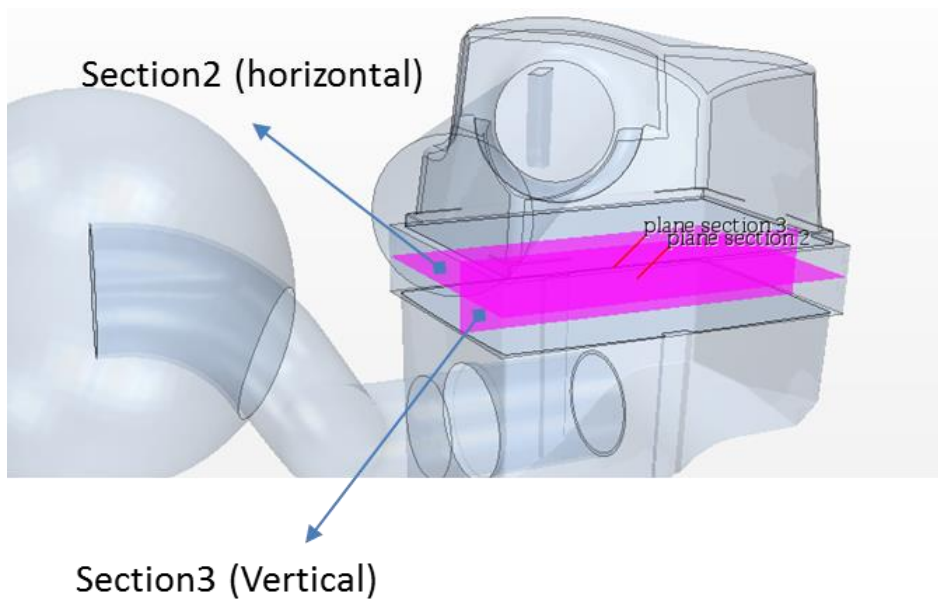Figure 3.33 shows velocity flow patterms from sections inside porous block as shown in Figure 3.32
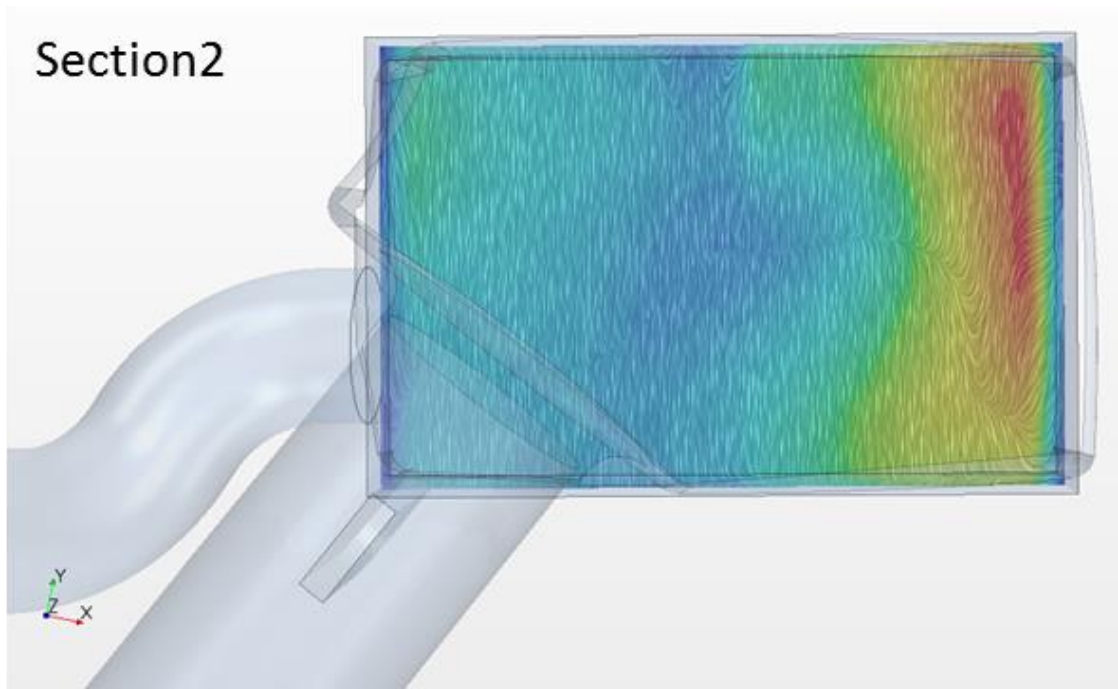

Figure 3.32 : Positions of sections 2 and 3

Figure 3.33 : Velocity contour as projected on section 2

Velocity scene is set up to show tangential velocity contours on middle section. As can be seen from the figure 3.33, flow is dominant in the parallel to the pleats direction. That is an expected phenomenon due to the fact that fluid encounters less resistance in parallel to the pleats direction.Figure 3.34 shows tangential velocity contour on section3.
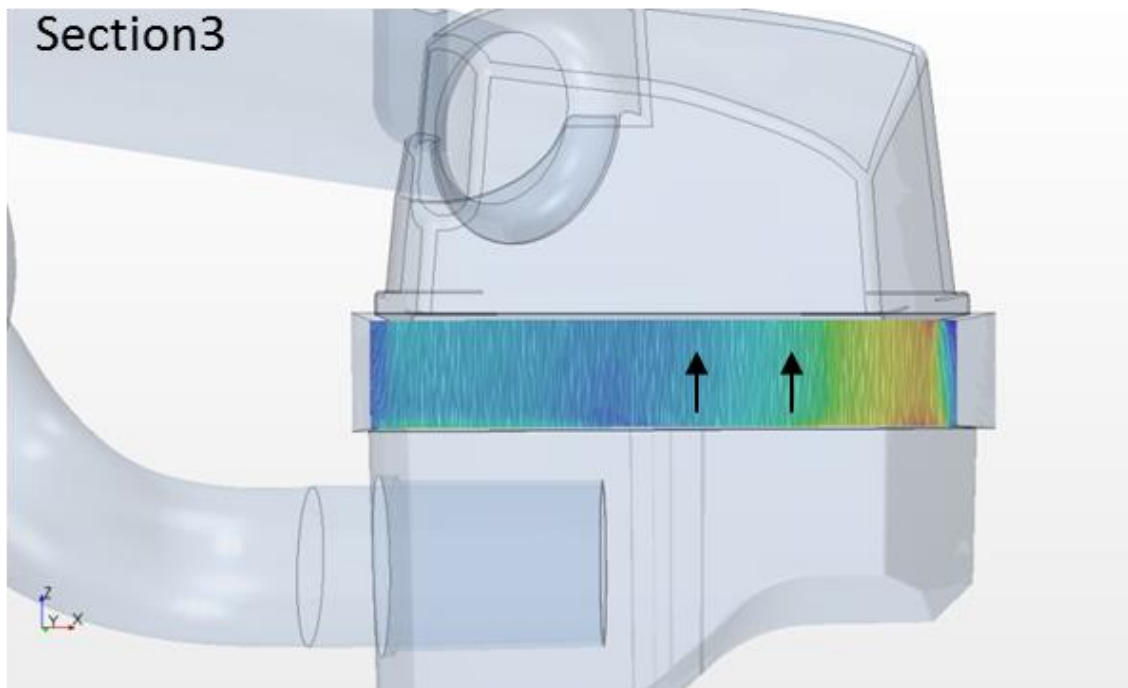

Figure 3.34 : Velocity contour as projected on section 3

Velocity, as can be seen in the figure 3.34, is dominant on the perpendicular to the pleats direction. It is again an expected phenomenon since this direction has less resistance than against the pleats direction. The velocity component on against the pleats direction is almost zero compared to the one in perpendicular to the pleats direction.

Flow uniformity upstream from mass flow sensor is also an important parameter for flow behavior. Surface Uniformity is a measure of velocity distribution and causes mass flow rate sensor to operate correctly and read data in a repeatable manner in real time.

Figures 5.15 and 5.16 show velocity contours upstream and downstream from mass flow rate sensor where Figure 3.35 shows position of mass flow sensor with respect to entire AIS.
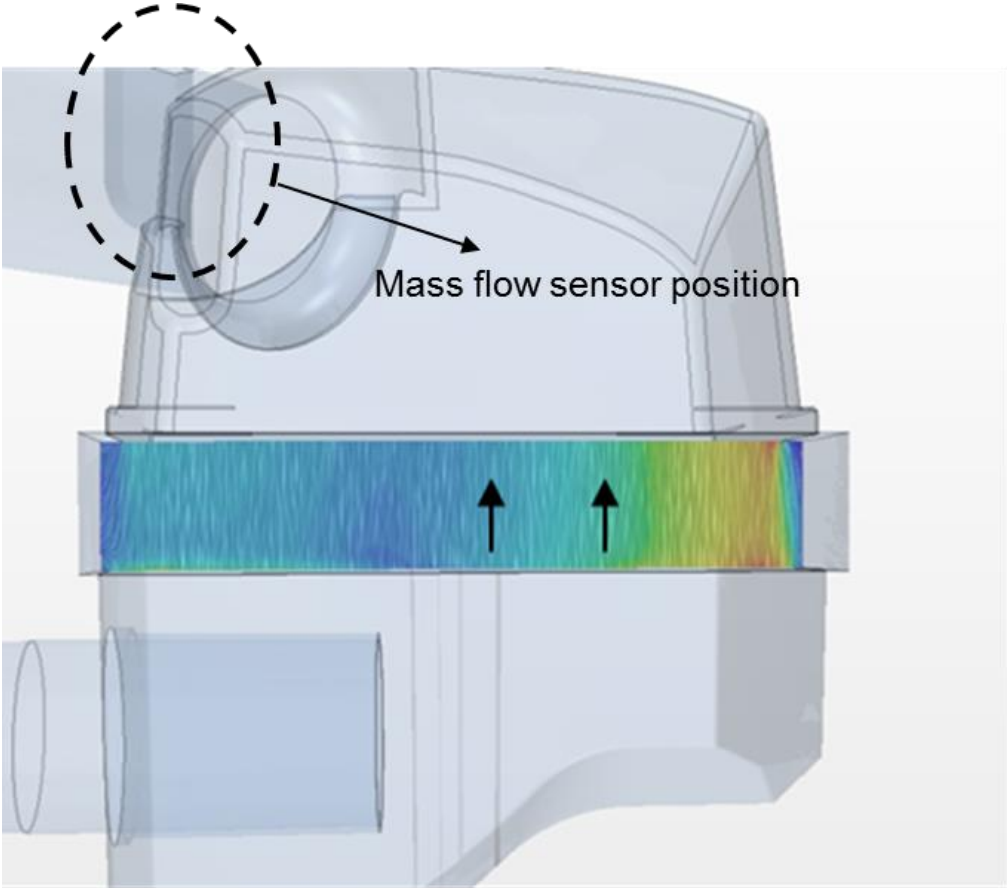

Figure 3.35 : Mass flow rate sensor position

Figure 3.36 and Figure 3.37 shows the velocity contours and surface uniformity values of upstream and downstream of mass flow sensor, respectively.

Velocity contours 5 mm upstream from mass flow sensor,
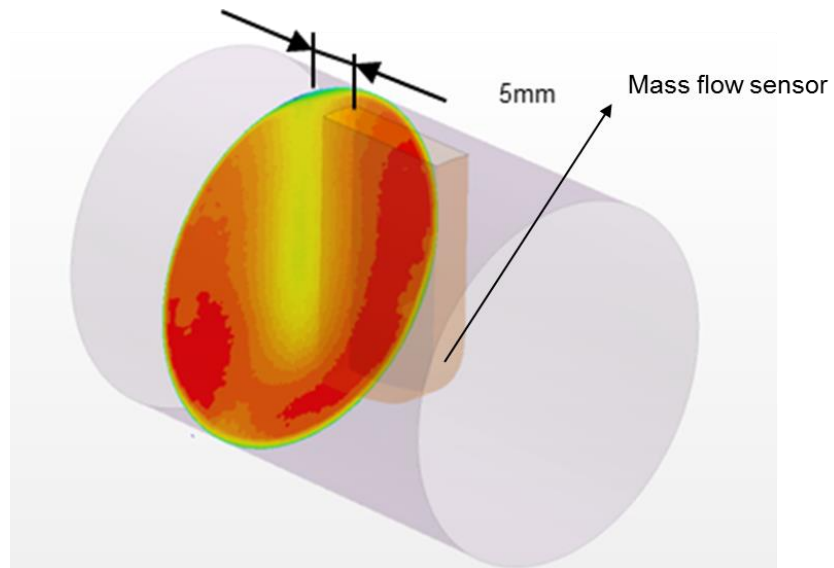
Surface Uniformity : 0.954

Figure 3.36 : Mass flow rate sensor position

Velocity contours 10 mm downstream from mass flow sensor,
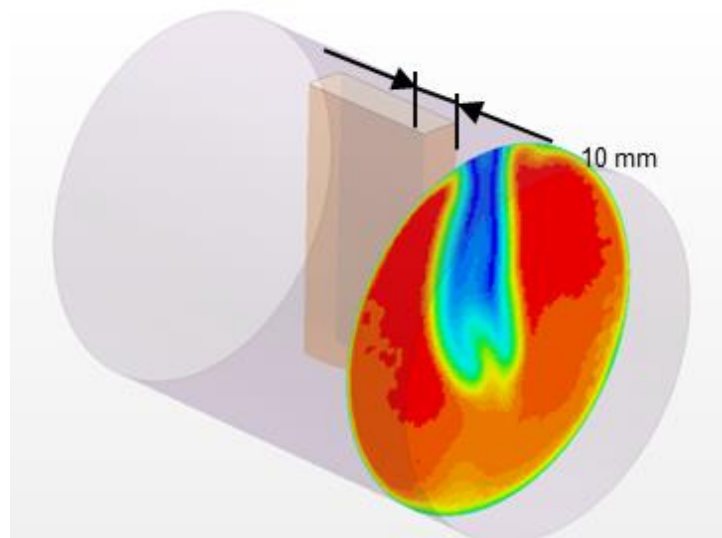
Surface Uniformity : 0.852

Figure 3.37 : Mass flow rate sensor position

3.5 Step 4: System Level Validation Test for AIS

To indicate CFD model's fidelty, a series of tests are conducted. Results are collected and provided in comparison at Results and Discussion section.

3.5.1 Air filter pressure drop test method

To assess air filter pressure drop, an internally standardized procedure is followed in Ford Otosan. A schematic view and a photograph of actual of test setup is provided in the Figure 3.38 and 3.39:
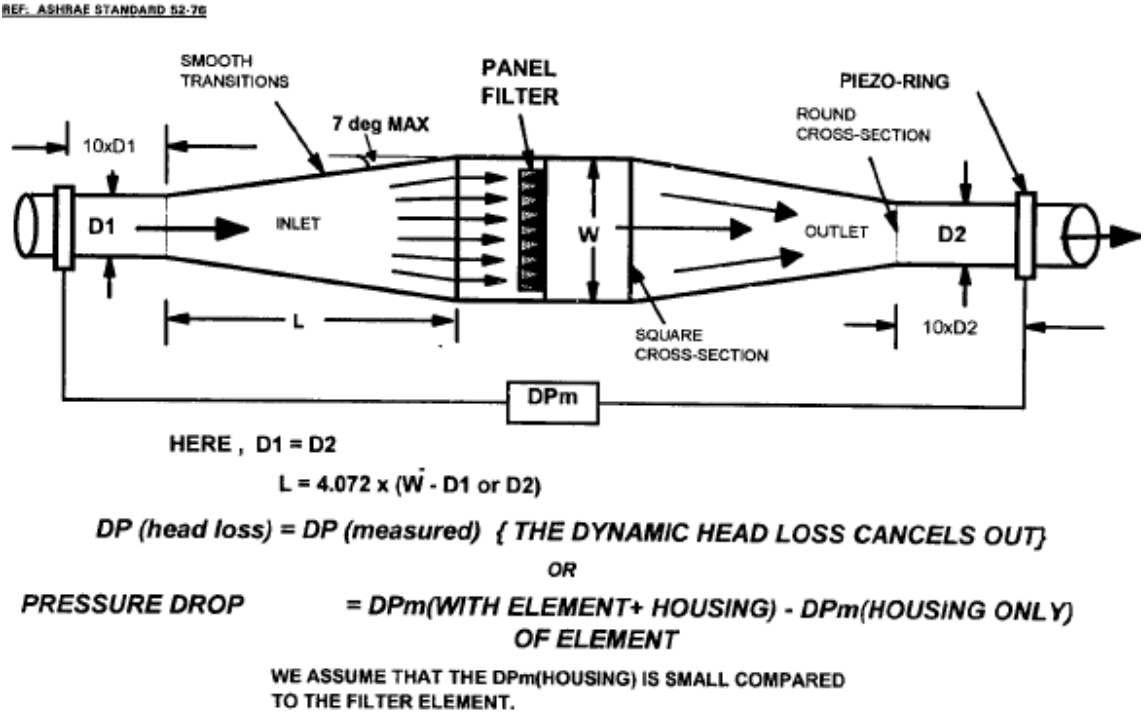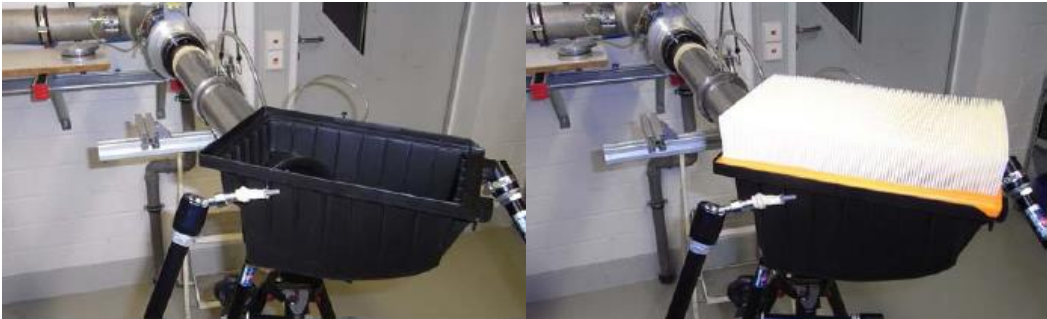

Figure 3.38 : Schematic image for test setup

Figure 3.39 : Test setup images

Method basically has the following steps:

1) Install Airbox assembly and pertinent cleanside and dirtyside ducts

2) Calibrate flow measurement devices

3) Adjust the mass flow rate to the maximum flow rate that occurs/expected to be occuring during engine operation.

4) Take measurement with filter element installed

5) Repeat the measurement to cover repeatability

6) Remove filter element from the assembly and repeat measurement

7) Repeat the measurements to cover repeatability.

Results collected for 7 different air filters to cover difference between provided parts.

Variation among measurements are all below 2%

3.5.2 AIS Pressure drop test method

For validation of this study, air filter pressure drop test is conducted with increased number of piezo-rings to have a better comparison of values predicted via CFD and actual values.

For validation of this study, air filter pressure drop test is conducted with increased number of piezo-rings to have a better comparison of values predicted via CFD and actual values.A schematic view and a photograph of actual of test setup is provided in the Figure 3.40 and 3.41:
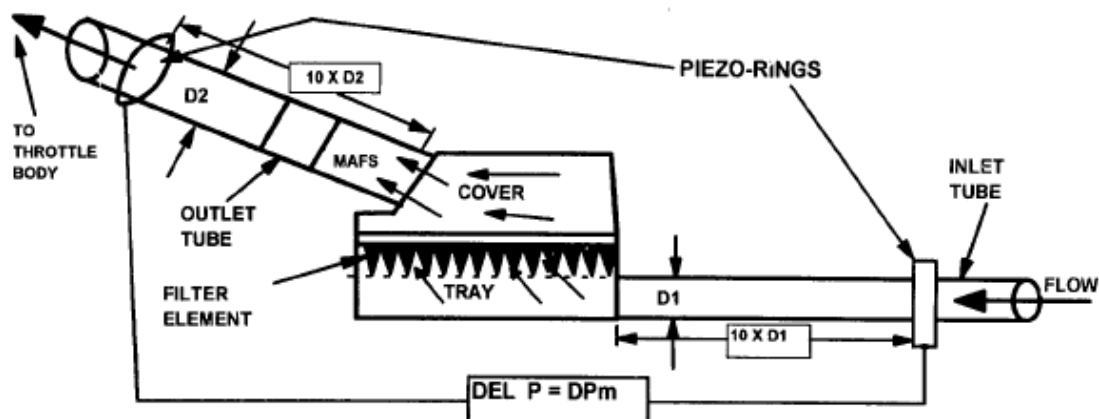

Figure 3.40 : Schematic test setup for geometry equivalent to main CFD model
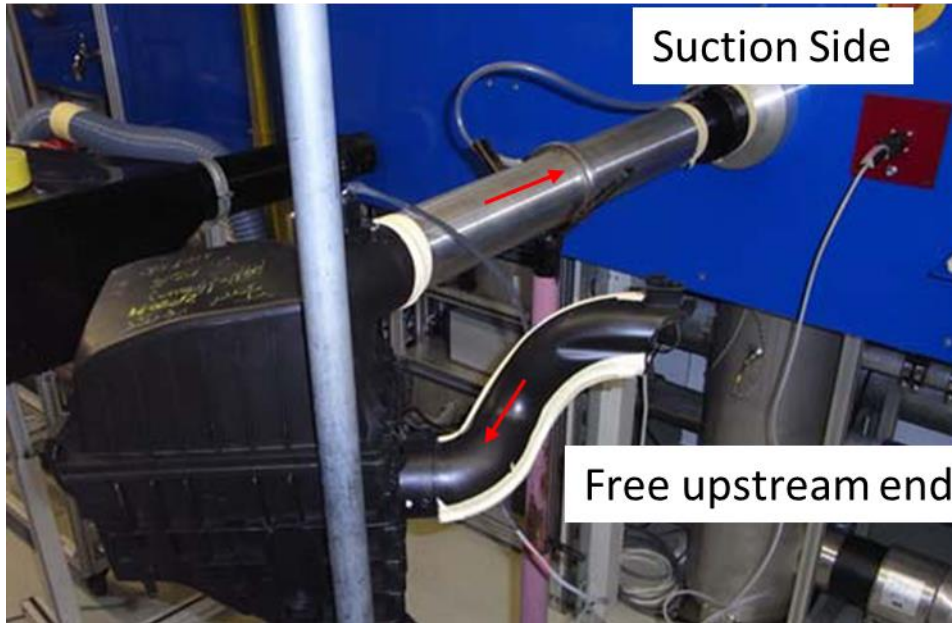
Figure 3.41 : Test setup images for geometry equivalent to main CFD model

Mass flow is created with suction from downstream side and dirtyside duct's upstream end is left free to make Test and CFD aligned. After instrumentation most of the sections marked in CFD model is instrumented in the test as well.

3.5.3 Comparison of Test Results with CFD

Upon completion of analyses, pressure drop of AIS is evaluated. Under same operation conditions, a test data acquired from Ford Otosan, regarding same geometry. Results are given in comparison in table 3.11. and figure 3.42. Please note that pressure drop values are scaled and presented as percentages section by section.

Table 3.11 : Predicted and tested pressure drop values AIS CFD

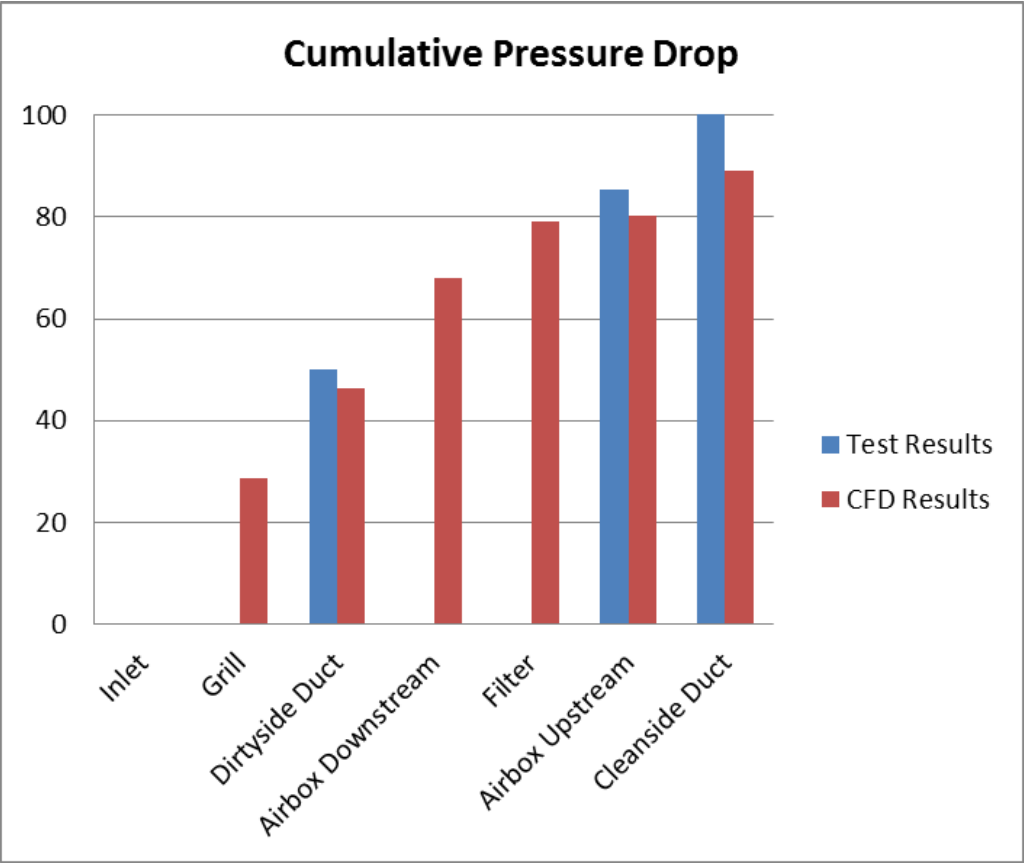| | ΔP Scaled to total ΔP level of system (%) | | | |
| | Test Results | | CFD Results | |
	Elementary	Cumulative	Elementary	Cumulative
Inlet			0	0.00
Grill			28.70	28.70
Dirtyside Duct		50.52±1.1	17.70	46.40
Airbox Downstream			21.52	67.92
Filter	**13.02±0.1**		**11.08**	**79.00**
Airbox Upstream		85.42±1.7	1.33	80.33
Cleanside Duct		100.00±1.9	11.67	89.00

Figure 3.42 : Column Chart for cumulative pressure drop

4. CONCLUSIONS AND RECOMMENDATIONS

Study is completed with derivation and validation of a method to model air filter element in less time and resource consuming CFD model, which has significant value in automotive industry.

Outcomes and commentary of the study can be summarized as follows:

- ASTM F778 test is reproduced via CFD, calculating air filter element's pressure loss with less than 7% difference in comparison with measurement.
- CFD analysis of AIS is underpredicting the pressure loss by 11% when compared to tests.
- CFD analysis of AIS underpredicts the pressure loss value around 15% for pleated air filter element when compared to measurement data.
- It is proven that accurracy of an AIS CFD analysis can be improved with relatively physical modelling of filter element.
- For correctous modelling of filter element, standard datasheet information of filter element is adequate.
- Accurracy of CFD model can be acceptable for early phases of design, but can not be trusted for product validation.
- Applying this procedure in design phase, is useful for prediction of flow behavior at compressor inlet and significantly lowers the amount of funds spent on test expenses for design iterations.

For studies to be done in future, scope of this project can be broadened by following additions:

- Filter element modelling can be extended to conical and cylindirical filter element configurations.
- Turbulence models or mesh quality can be improvedin order to incease the level of accurracy at the expense of computational labor.

- The process can be automatized with scripts formed in java or other programming environments, or supported with a graphical user interface to prevent errors sourcing from program operator.

REFERENCES

[1] **EGR Systems and Components** (2011) in DieselNet Date retrieved : 03.05.2015

   https://www.dieselnet.com/tech/engine_egr_sys.php

[2] **Ford Motor Company Test Specs** (2011). in Rlis Date Retrieved : 07.06.2015
   https://www.rlis.ford.com/

[3] **Moreira, F., Costa, Anderson da S., Tamburi, L.E., Malagutti,R.** (2006). Three-dimensional Numerical Analysis of Flow inside an Automotive Air filter, SAE Technical Paper 2006-01-2629

[4] **Joshi, S. S., Mathews, V., Nandgaonkar, M., Kajale, S., Niranjan, M. Krishnan, S.** (2007). Application of CFD Methodology to Air Intake System of CRDI Engine, SAE Technical Paper 2007-01-3699

[5] **Huuderman, B. and Banzhaf, H.,** (2006). CFD Simulation of Flows in Air Cleaners with Transient Dust Loading of the Filter Element, SAE Technical Paper 2006-01-1316

[6] **Siqueira, C. L. R., Kessler, M. P., Moreira, F., Costa, A. S. Tamburi, L.E.,** (2006). Application of CFD Methodology to Air Intake System, SAE Technical Paper 2006-01-3678

[7] **Mamat, R., Mahrous, A. M., Xu, H., Wyszynski, M. L. Pierson, S., Qiao, J.,** (2008). Application of CFD Methodology to Air Intake System of CRDI Engine, SAE Technical Paper 2008-01-1643

[8] **Andersson, B., Andersson, R., Hakansson, L., Mortensen, M., Sudiyo, R. Wachem Chiang, S. T.,** (2012). Computational Fluid Dynamics for engineers, Cambridge University Press, 2012

[9] **StarCCM+ v.10.02 User Guide** (2015). In Steve Portal, Date Retrieved 30.06.2015   http://stevedocs.cd-adapco.com/ViewDocs/authdocs/starccmplus_latest_en/index.html

[10] **Vafai, K.,** (2005) Handbook of Porous Media, Taylor and Francis, New York

[11] **Zikanov, O.,** (2010).Essential Computational Fluid Dynamics, Wiley, 2010

[12] **ICEM CFD v.11.0 Tutorial,** (2012), ANSYS Inc.

[13] **ASTM F778** (2008).Testing standard for pure air permeability, ASTM

[14] **Mahle Product Catalogue** (2011)

CURRICULUM VITAE
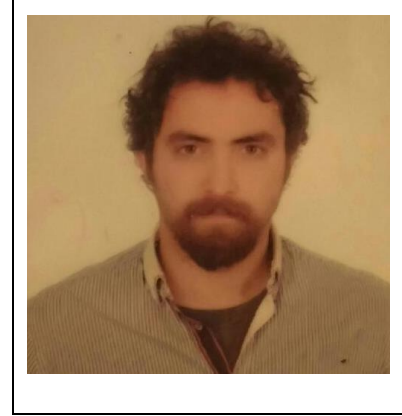
Name Surname: Anıl Can Ağar

Place and Date of Birth:İstanbul, 1988

E-Mail: agaran@itu.edu.tr

EDUCATION:

B.Sc.:İstanbul Technical University

PROFESSIONAL EXPERIENCE AND REWARDS:

- **Engineering Intern (June '09-June '10) :BSH Bosch and Siemens Home Appliances Group,** Participated in long term internship program in product development. Completed assigned projects including B.Eng thesis, which is conducted in collaboration between Istanbul Technical University and BSH. All projects finalized with complete fulfillment of deliverables specified.
- **3D Computational Fluid Dynamics Engineer (August '10-present):** Responsibilities include design, assessment and optimization of any automotive component in interaction with fluid flow. Delivered projects are in fields of Combustion, Air induction, Exhaust emission reduction and Cooling systems. Computer aided design of flow related components is also performed.Experience in company involves usage of wide variety of simulation tools such as StarCCM+, Converge, optimization tools as ModeFrontier, CAD tools as CATIA and SolidWorks. To enhance processes with programming and actively run simulations on High Performance Computing environment, Shell scripting and programming in Java are among the skills required to meet and exceed expectations.